LAWRENCE
LIVERMORE
NATIONAL
LABORATORY

LLNL-TR-727558

MODAL TRACKING of A Structural Device: A Subspace Identification Approach

J. V. Candy, S. N. Franco, E. L. Ruggiero, M. C. Emmons, I. M. Lopez, L. M. Stoops

March 23, 2017

Disclaimer

This work performed under the auspices of the U.S. Department of Energy by Lawrence Livermore National Laboratory under Contract DE-AC52-07NA27344.

MODAL TRACKING OF A STRUCTURAL DEVICE:

A Subspace Identification Approach

J. V. Candy, S. N. Franco, E. L. Ruggiero, M. C. Emmons, I. M. Lopez, L. M. Stoops

Executive Summary

Mechanical devices operating in an environment contaminated by noise, uncertainties, and extraneous disturbances lead to low signal-to-noise-ratios creating an extremely challenging processing problem. To detect/classify a device subsystem from noisy data, it is necessary to identify unique signatures or particular features. An obvious feature would be resonant (modal) frequencies emitted during its normal operation. In this report, we discuss a model-based approach to incorporate these physical features into a dynamic structure that can be used for such an identification. The approach we take after pre-processing the raw vibration data and removing any extraneous disturbances is to obtain a representation of the structurally unknown device along with its subsystems that capture these salient features. One approach is to recognize that unique modal frequencies (sinusoidal lines) appear in the estimated power spectrum that are solely characteristic of the device under investigation. Therefore, the objective of this effort is based on constructing a black box model of the device that captures these physical features that can be exploited to "diagnose" whether or not the particular device subsystem (track/detect/classify) is operating normally from noisy vibrational data. Here we discuss the application of a modern system identification approach based on stochastic subspace realization techniques capable of both (1) identifying the underlying black-box structure thereby enabling the extraction of structural modes that can be used for analysis and modal tracking as well as (2) indicators of condition and possible changes from normal operation.

Typically, the vibrational signature of the structural device is measured (directly or remotely) and provided as a noisy input to a modal identifier that is used to track modal evolution as well as construct a decision function as input to a detector. The detector first "decides" whether or not it is potentially an anomalous structural subsystem that is not vibrating normally. If so, the detector provides an input to the device classifier to decide on the particular class or sub-

system anomaly. In this paper, we confine our focus on the modal identification and tracking aspects of the anomaly detection problem.

We briefly develop the necessary background in stochastic subspace realization, discuss the algorithm and apply it to an unknown structural device (black box) characterized by a set of noisy multiple input/multiple output accelerometer measurements extracting the modal model from buffered segments of data, extract the unique modal frequencies, track their evolution and evaluate the overall performance of the processor.

1.0 INTRODUCTION

Complex mechanical devices operating in environments contaminated by noise, uncertainties, and extraneous disturbances lead to low signal-to-noise-ratios creating an extremely challenging processing problem to: (1) detect that they are operating "normally"; and (2) determine critical subsystem performance, that is, their identities, location and overall condition. In attempting to detect/classify a particular type of device subsystem from noisy vibration data, it is necessary to identify signatures or particular features from that device that make it unique. One of the most obvious features would be to identify resonant (modal) frequencies emitted during its normal operation. In this report, we discuss a model-based approach to incorporate these physical features into a dynamic structure that can be used for such an identification. The approach we take after pre-processing the raw vibration data and removing any extraneous disturbances is to obtain a representation of the structurally unknown device along with its subsystems that capture these salient features.

Many applications require the monitoring of structural modes to determine the condition of a device under investigation especially if the it is a critical entity of an operational system. For instance, a cooling pump of a nuclear reactor on a submarine or surface ship or the structural integrity of the hull of a sea going vessel after an event may have occurred that has possibly altered its integrity. Application to a wide variety of on-board engines or motors of ships as well as autonomous underwater vehicles require constant monitoring especially prior-to and during at-sea applications. Here

we discuss the application of a modern system identification approach based on stochastic subspace realization techniques capable of both (1) identifying the underlying black-box structure thereby enabling the extraction of structural modes that can be used for analysis and modal tracking as well as (2) indicators of condition and possible changes from normal operation.

One approach is to recognize that unique modal frequencies (e.g. sinusoidal lines) appear in the estimated power spectrum that are solely characteristic of the device under investigation. Therefore, the objective of this effort is based on constructing a black box model of the device that captures these physical features that can be exploited to "diagnose" whether or not the particular device subsystem (track/detect/classify) is operating normally from noisy vibrational data. Standard approaches to detect anomaly mechanisms at the onset range from a simple accelerometer strategically placed to observe the Fourier spectrum of known response to using cepstral analysis to identify periodic responses. Measures of anomalies can deteriorate significantly if noise is present - a common situation in an operational environment. Most of the current monitoring approaches for anomaly detection and isolation lead to single-channel processing of measured sensor data. Multiple sensors (such as accelerometers for vibrations, microphones for acoustics, strain gauges for stress and thermocouples for temperature) in a structure provide additional information about the system for condition and performance. This implies that the application of a multi-channel (multi-input, multi-output) system representation, which is most easily handled in state-space form, without restrictions to single-channel spectral representations is required.

The approach we take is outlined in the figure below. A model-based modal detection scheme for device diagnostics is illustrated conceptually in Fig. 1.0. Here the vibrational signature of the structurally unknown device is measured (directly or remotely) and provided as a noisy input to a modal identifier that is used to track modal evolution as well as construct a decision function as input to a detector. The detector first "decides" whether or not it is potentially an anomalous structural subsystem that is not vibrating normally. If so, it provides an input to the device classifier to decide on the particular class or subsystem anomaly. In this report, we confine our focus on the modal identification and tracking aspects of the anomaly detection problem.

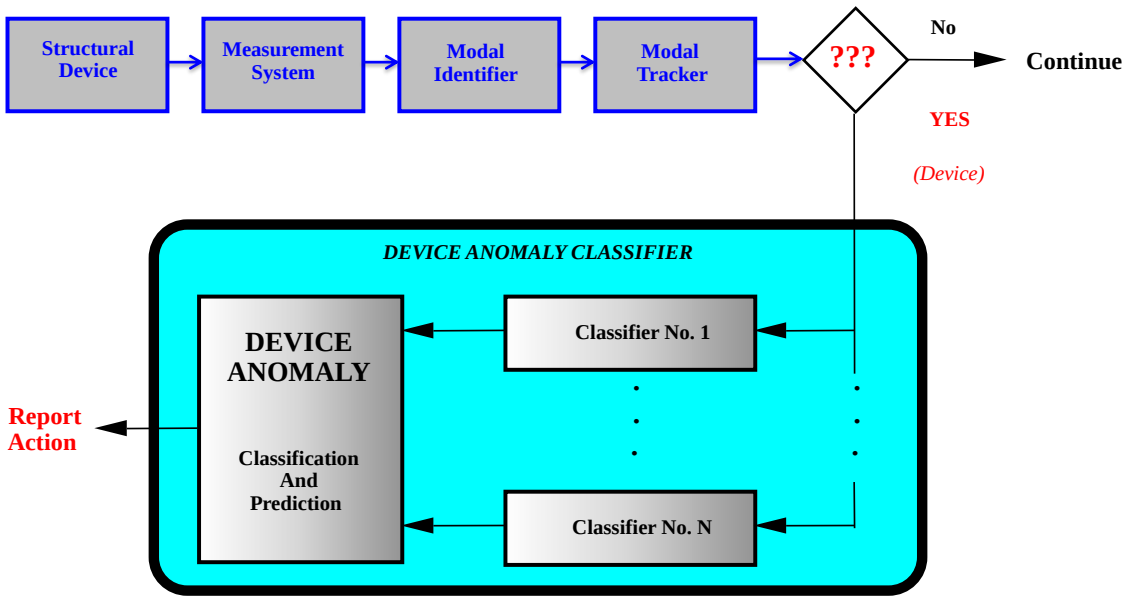

Figure 1: Conceptual model-based detection scheme: vibration measurement system, modal identifier (subspace realization) modal tracker/detector with subsequent device classifier.

The model-based approach for anomaly detection, classification and prediction was shown in Fig. 1.0. The basic concept is that the process or vibrational system under consideration is modeled using system identification techniques [1], [2] to "fit" modal models to the data. If direct noise data is not available, then a reasonable approach is to model the noise as additive and random leading to a Gauss-Markov model [1]. Once a representation of the overall system (structure, sensors, and noise) is developed, then a anomaly detector or condition monitor can be developed to monitor the status of the dynamic vibrational system.

We briefly develop the necessary background in stochastic subspace realization, discuss the algorithm and apply it to an unknown structural device (black box) characterized by a set of noisy multiple input/multiple output accelerometer measurements extracting the modal model from buffered segments of data and evaluate its overall performance. Our goal is to eventually provide a real-time technique for on-board processing.

2.0 State-Space Vibrational Models

Most structures or equivalently vibrational systems are multiple input/multiple output (*MIMO*) systems that are easily captured within the state-space framework. For instance, a linear, time-invariant mechanical system can be expressed as a second order vector-matrix, differential equation given by

$$M\ddot{\mathbf{d}}(\tau) + C_d\dot{\mathbf{d}}(\tau) + K\mathbf{d}(\tau) = B_p\mathbf{p}(\tau) \tag{1}$$

where $\mathbf{d}$ is the $N_d \times 1$ displacement vector, $\mathbf{p}$ is the $N_p \times 1$ excitation force, and M, C_d, K, are the $N_d \times N_d$ lumped mass, damping, and spring constant matrices characterizing the vibrational process model, respectively.

Defining the $2N_d$-state vector in terms of the displacement and its derivative as $\mathbf{x}(\tau) := \left[\begin{array}{c|c} \mathbf{d}(\tau) & \dot{\mathbf{d}}(\tau) \end{array}\right]$, then the continuous-time state-space representation of this process can be expressed as

$$\dot{\mathbf{x}}(\tau) = \underbrace{\left[\begin{array}{c|c} 0 & I \\ \hline -M^{-1}K & -M^{-1}C_d \end{array}\right]}_{A}\mathbf{x}(\tau) + \underbrace{\left[\begin{array}{c} 0 \\ \hline M^{-1}B_p \end{array}\right]}_{B}\mathbf{p}(t) \tag{2}$$

The corresponding measurement or output vector relation can be characterized by

$$\mathbf{y}(\tau) = \mathbf{C_a}\ddot{\mathbf{d}}(\tau) + \mathbf{C_v}\dot{\mathbf{d}}(\tau) + \mathbf{C_d}\mathbf{d}(\tau) \tag{3}$$

where the constant matrices: $\mathbf{C_a}, \mathbf{C_v}, \mathbf{C_d}$ are the respective acceleration, velocity and displacement weighting matrices of appropriate dimension.

In terms of the state vector relations of Eq. 2, we can express the acceleration vector as:

$$\ddot{\mathbf{d}}(\tau) = -M^{-1}K\mathbf{d}(\tau) - M^{-1}C_d\dot{\mathbf{d}}(\tau) + M^{-1}B_p\mathbf{p}(\tau) \tag{4}$$

Substituting for the acceleration term in Eq. 3, we have that

$$\mathbf{y}(\tau) = -\mathbf{C_a}M^{-1}\Big[B_p\mathbf{p}(\tau) - C_d\dot{\mathbf{d}}(\tau) - K\mathbf{d}(\tau)\Big] + \mathbf{C_v}\dot{\mathbf{d}}(\tau) + \mathbf{C_d}\mathbf{d}(\tau)$$

or

$$\mathbf{y}(\tau) = \underbrace{\Big[C_d - \mathbf{C_a}M^{-1}K \;\Big|\; \mathbf{C_v} - \mathbf{C_a}M^{-1}C_d\Big]}_{C} \left[\begin{array}{c} \mathbf{d}(\tau) \\ - - - \\ \dot{\mathbf{d}}(\tau \end{array}\right] + \underbrace{\mathbf{C_a}M^{-1}B_p}_{D}\mathbf{p}(\tau) \tag{5}$$

to yield the vibrational measurement as:

$$\mathbf{y}(\tau) = C\mathbf{x}(\tau) + D\mathbf{u}(\tau) \tag{6}$$

where the output or measurement vector is $\mathbf{y} \in \mathcal{R}^{N_y \times 1}$ completing the multiple input/multiple output (MIMO) vibrational model.

Note that sensor models can capture the dynamics of the sensors, as they interact with the dynamics of the states. For example, in a typical vibrational system, this equation represents the outputs of a set of accelerometers which are wideband relative to the process and therefore, simply fixed gains.

One of the most expository representations of a mechanical system is its modal representation [3], [4], where the modes and mode shape expose the internal structure and its response to various excitations. The modal representation of a system can easily be found from state-space systems by transforming the coordinates of the representation to modal space which

is accomplished through an eigen-decomposition in the form of a *similarity transformation* such that the system matrices $\Sigma := \{A, B, C, D\}$ are transformed to modal coordinates by the transformation matrix T_M constructed of the eigenvectors of the underlying system [5], [6] ,[7], that is,

$$\Sigma \quad \overset{T_M}{\longrightarrow} \quad \Sigma_M$$

where we have

$$\Big\{A, B, C, D\Big\} \longrightarrow \Big\{A_M, B_M, C_M, D_M\Big\} := \Big\{T_M A T_M^{-1}\ , T_M B,\ C T_M^{-1}, D\Big\}$$

that yields an "equivalent" system from an input/output perspective, that is, the transfer functions are identical

$$H(s) = C_M(sI - A_M)^{-1}B_M + D_M = CT_M^{-1} \times (sI - T_M A T_M^{-1})^{-1} \times T_M B = C(sI - A)^{-1}B + D$$

as well as the corresponding impulse response matrices

$$H(\tau) = C_M e^{A_M(\tau)} B_M = CT_M^{-1} \times T_M e^{A(\tau)} T_M^{-1} \times T_M B = Ce^{A(\tau)}B$$

It is well-known from systems theory [5]-[7] that the solution to the continuous-time, state-space system of Eq. 2 is given by

$$\mathbf{x}(\tau) = \underbrace{e^{A(\tau-\tau_0)}\mathbf{x}(\tau_0)}_{\text{homogeneous}} + \underbrace{\int_{\tau_0}^{\tau} e^{A(\tau-\alpha)} B\mathbf{u}(\alpha) d\alpha}_{\text{forced}} \tag{7}$$

consisting of the homogeneous and forced solutions from which can define the *state transition matrix* for the linear time invariant (LTI) system as

$$\mathbf{\Phi}(\tau, \tau_0) = e^{A(\tau-\tau_0)} \qquad \text{[State Transition Matrix]} \tag{8}$$

Transforming this solution by performing an eigen-decomposition for distinct (independent) eigenvalues leads to a diagonal transition matrix, that is, selecting the modal similarity transformation T_M for

$$x(\tau) = T_M \times x_M(\tau)$$

satisfying the eigen-equations

$$A\varepsilon_i = \lambda_i \varepsilon_i \qquad \text{for} \qquad i = 1, 2, \cdots, N_x$$

where $\{\lambda_i\}$ are the distinct eigenvalues (real and/or complex) of A or equivalently the roots (modes) of the determinant $|\lambda I - A|$ (characteristic equation) [13] and $\{\varepsilon_i\}$ are the corresponding eigenvectors (mode shapes) that lead to

$$T_M = [\varepsilon_1 \mid \varepsilon_2 \mid \cdots \mid \varepsilon_{N_x}]$$

the *modal matrix* consisting of independent columns such that

$$AT_M = T_M \Lambda$$

for $\Lambda = \text{diag}[\lambda_1, \lambda_2, \cdots, \lambda_{N_x}]$.

For this modal system, we have that the *modal* state transition matrix $\mathbf{\Phi}_M$ follows from the eigen-decomposition as

$$\mathbf{\Phi}_M(\tau, \tau_0) = T_M e^{A(\tau-\tau_0)} T_M^{-1} = e^{T_M A(\tau-\tau_0)T_M^{-1}} = e^{\Lambda(\tau-\tau_0)} = \sum_{i=1}^{N_x} \varepsilon_i e^{\lambda_i(\tau-\tau_0)} \eta_i^T \tag{9}$$

where we have incorporated the *reciprocal eigenvectors*s $\{\eta_i^T\};\ i = 1, \cdots, N_x$ (rows of T_M^{-1}) to obtain

$$\mathbf{\Phi}_M(\tau, \tau_0) = e^{\Lambda(\tau-\tau_0)} = \begin{bmatrix} e^{\lambda_1(\tau-\tau_0)} & & 0 \\ & \ddots & \\ 0 & & e^{\lambda_{N_x}(\tau-\tau_0)} \end{bmatrix} \quad \text{[MODAL State Transition Matrix]} \tag{10}$$

In this coordinate system, the *modal* state solution is:

$$\mathbf{x}_M(\tau) = e^{\Lambda(\tau-\tau_0)} \mathbf{x}_M(\tau_0) + \int_{\tau_0}^{\tau} e^{\Lambda(\tau-\alpha)} B\mathbf{u}(\alpha) d\alpha \tag{11}$$

which can be written explicitly for the i^{th}-mode x_i as

$$x_i(\tau) = e^{\lambda_i(\tau-\tau_0)} x_i(\tau_0) + \int_{\tau_0}^{\tau} e^{\lambda_i(\tau-\alpha)} b_{im} u_m(\alpha) d\alpha \tag{12}$$

for $i = 1, 2, \cdots, N_x; m = 1, \cdots, N_u$ with b_{im} the $(i, m)^{th}$ component of the input transmission matrix B.

The corresponding measurement or output of the state-space system is easily found by multiplying Eq. 7 by the measurement matrix C, that is,

$$\mathbf{y}_M(\tau) = C_M e^{\Lambda(\tau-\tau_0)}\mathbf{x}(\tau_0) + \int_{\tau_0}^{\tau} C_M e^{\Lambda(\tau-\alpha)} B_M \mathbf{u}(\alpha) d\alpha \tag{13}$$

which can also be expressed by applying the modal transformation as to obtain the m^{th}-component of the output y_m as

$$y_n(\tau) = \sum_{i=1}^{N_x} c_{ni}^T e^{\lambda_i(\tau-\tau_0)}\, x_i(\tau_0) + \sum_{i=1}^{N_x} \int_{\tau_0}^{\tau} c_{ni} e^{\lambda_i(\tau-\alpha)}\, b_{im} u_m(\alpha) d\alpha \text{ for } n = 1, \cdots, N_y \tag{14}$$

with c_{ni} the $(n, i)^{th}$ component of the of output transmission matrix C. This is defined as the *modal representation* of the system [6].

With this in mind, we now extend the *modal state-space system* to the complex modal case which is quite common in structural dynamics [3], [4]. For a typical structural system, the eigenvalues are complex, but still distinct. In this case the system matrix can be decomposed, as before, using the eigen-decomposition which now yields complex eigen-pairs along with the corresponding complex eigenvectors, that is,

$$\begin{aligned} \lambda_i &= -\sigma_i \pm j\omega_i \\ \mathbf{t}_i &= [\xi_i \mid \xi_i^*] \quad \text{for} \quad i = 1, 2, \cdots, N_d \text{ for } N_x = 2 \times N_d \end{aligned} \tag{15}$$

for N_d the dimension of the corresponding displacement vector of Eq. 1 and $\mathbf{t}_i$ the i^{th}-column vector of T_M with σ_i is the *damping coefficient*, ω_i the *damped natural frequency* and ϕ_i the *phase* (see Sec. 2.0) such that

$$e^{-\sigma_i \tau} \times \cos(\omega_i \tau + \phi_i) \qquad \text{[Damped Sinusoid]}$$

Note that the *homogeneous* state and output responses are *real*, since

$$\mathbf{x}_M(\tau) = \sum_{i=1}^{N_x} 2e^{-\sigma_i(\tau-\tau_0)} \Re\{\mathbf{x}_i(\tau_0)\} = \sum_{i=1}^{N_x} 2e^{-\sigma_i(\tau-\tau_0)} |\mathbf{x}_i(\tau_0)| \cos(\omega_i \tau + \phi_i) \tag{16}$$

We also have that the modal transformation matrix becomes

$$T_M = \left[\xi_1 \; \xi_1^* \mid \xi_2 \; \xi_2^* \mid \; \cdots \; \mid \xi_{N_x/2} \; \xi_{N_x/2}^* \mid \right] \tag{17}$$

and applying this transformation to the system matrix A, we obtain

$$A_M = \Lambda = T_M \times A \times T_M^{-1} = \text{diag}\left(\left[\begin{array}{cc} \sigma_1 & \omega_1 \\ -\omega_1 & \sigma_1 \end{array}\right], \cdots, \left[\begin{array}{cc} \sigma_{N_x} & \omega_{N_x} \\ -\omega_{N_x} & \sigma_{N_x} \end{array}\right]\right) \tag{18}$$

with

$$B_M = T_M \times B; C_M = C \times T_M^{-1} \qquad \text{and} \qquad D_M = D$$

which leads to the modal state transition matrix for the complex eigen-system as

$$\Phi_M(\tau, \tau_0) = e^{\Lambda(\tau-\tau_0)} = \exp\left\{\underbrace{\left[\begin{array}{ccc} \Lambda_1 & & 0 \\ & \ddots & \\ 0 & & \Lambda_{Nx} \end{array}\right]}_{\Lambda}(\tau - \tau_0)\right\} \text{ for } \Lambda_i = \left[\begin{array}{cc} \sigma_i & \omega_i \\ -\omega_i & \sigma_i \end{array}\right] \tag{19}$$

Thus, the complex modal state-space system is given by

$$\begin{array}{rcl} \dot{\mathbf{x}}(\tau) & = & A_M\mathbf{x}(\tau) + B_M\mathbf{u}(\tau) \\ \mathbf{y}(\tau) & = & C_M\mathbf{x}(\tau) + D_M\mathbf{u}(\tau) \end{array} \tag{20}$$

where the system matrices become

$$A_M = \left[\begin{array}{cccc} A_{M_1} & 0 & \cdots & 0 \\ 0 & A_{M_2} & \cdots & 0 \\ \vdots & \vdots & \ddots & 0 \\ 0 & 0 & \cdots & A_{M_{N_x}} \end{array}\right]$$

$$B_M = \left[\begin{array}{c} B_{M_1} \\ \vdots \\ B_{M_{N_x}} \end{array}\right]; \; C_M = \left[C_{M_1} \mid \cdots \mid C_{M_{N_x}}\right]; \; D_M = D$$

and $A_{M_i} = \Lambda_i$.

Sampling this system with an analog-to-digital converter (ADC) such that $\tau \to t_k$ over the interval $(\tau_k, \tau_{k-1}]$, then we have the corresponding *sampling interval* defined by $\triangle t_k := \tau_k - \tau_{k-1}$.

$$x(t_k) = \Phi(t_k, t_{k-1})x(t_{k-1}) + \int_{t_{k-1}}^{t_k} \Phi(t_k, \alpha)B_c(\alpha)u_\alpha d\alpha \tag{21}$$

and therefore from the differential equation above, we have the solution

$$\Phi(t_k, t_{k-1}) = \int_{t_{k-1}}^{t_k} A(\alpha)\Phi(t_k, \alpha)d\alpha \qquad \text{for} \qquad \Phi(t_0, t_0) = I \tag{22}$$

where $\Phi(t_k, t_{k-1})$ is the *sampled-data* state transition matrix—the critical component in the solution of the state equations enabling us to calculate the state evolution in time.

If we further assume that the input excitation is *piecewise constant* ($u_\alpha \to u(t_{k-1})$) over the interval $(t_k, t_{k-1}]$, then it can be removed from under the superposition integral in Eq. 21 to give

$$x(t_k) = \Phi(t_k, t_{k-1})x(t_{k-1}) + \left(\int_{t_{k-1}}^{t_k} \Phi(t_k, \alpha)B_c(\alpha)d\alpha\right) \times u(t_{k-1}) \tag{23}$$

Under this assumption, we can define the sampled *input transmission* matrix as

$$B(t_{k-1}) := \int_{t_{k-1}}^{t_k} \Phi(t_k, \alpha)B_c(\alpha)d\alpha \tag{24}$$

and therefore the *sampled-data state-space system* with equally or unequally sampled data is given by:

$$\begin{aligned} x(t_k) &= \Phi(t_k, t_{k-1})x(t_{k-1}) + B(t_{k-1})u(t_{k-1}) \\ y(t_k) &= C(t_k)x(t_k) + D(t_k)u(t_k) \end{aligned} \tag{25}$$

For a discrete-time LTI system (to follow), it is straightforward to show by induction that [1]

$$\Phi(t,\ell) = A^{t-\ell} \tag{26}$$

Since we sample the continuous-time system, we will employ a discrete state-space representation and then transform the results back to the continuous-time domain. The generic linear, time invariant *state-space* model is defined by its system matrix A, input transmission matrix B, output or measurement matrix C and direct input feed-through matrix D for *discrete-time* systems as

$$\begin{aligned} x(t+1) &= Ax(t) + Bu(t) && \text{[State]} \\ y(t) &= Cx(t) + Du(t) && \text{[Output]} \end{aligned} \tag{27}$$

for the state $x \in R^{N_x \times 1}$, input $u \in R^{N_u \times 1}$, and output $y \in R^{N_y \times 1}$ with t an integer.

Corresponding to this representation is the discrete *transfer function* in terms of the Z-transform

$$H(z) = C(zI - A)^{-1}B + D \tag{28}$$

and the corresponding *impulse response* termed the Markov parameters [5], [7]

$$H(t) = CA^{t-1}B + D\delta(t) \tag{29}$$

for δ the Kronecker delta function.

Expanding the state equations, we can easily show that

$$x(t) = A^t x(0) + \sum_{k=0}^{t-1} A^{t-k-1}Bu(k-1); \qquad t = 0, 1, \cdots, K \tag{30}$$

and therefore the output is given by

$$y(t) = CA^t x(0) + \sum_{k=0}^{t-1} CA^{t-k-1}Bu(k-1) + D\delta(t) \tag{31}$$

or expanding this relation further, we have

$$\begin{bmatrix} y(0) \\ y(1) \\ \vdots \\ y(K-1) \end{bmatrix} = \underbrace{\begin{bmatrix} C \\ CA \\ \vdots \\ CA^{t-K-1} \end{bmatrix}}_{\mathcal{O}} x(0) + \underbrace{\begin{bmatrix} D & & \cdots & 0 \\ CB & D & \cdots & 0 \\ \vdots & \vdots & \vdots & \vdots \\ CA^{K-1}B & \cdots & CB & D \end{bmatrix}}_{\mathcal{T}} \begin{bmatrix} u(0) \\ u(1) \\ \vdots \\ u(K-1) \end{bmatrix} \tag{32}$$

Shifting these relations in time is simply given by

$$\begin{bmatrix} y(\ell) \\ y(\ell+1) \\ \vdots \\ y(\ell+K-1) \end{bmatrix} = \mathcal{O}_K x(0) + \mathcal{T}_K \begin{bmatrix} u(\ell) \\ u(\ell+1) \\ \vdots \\ u(\ell+K-1) \end{bmatrix} \tag{33}$$

$$y_K(\ell) = \mathcal{O}_K x(\ell) + \mathcal{T}_K u_K(\ell) \tag{34}$$

where $\mathcal{O}$ is the *observability matrix* of linear systems theory [1].

Now if we combine these m of these vectors of Eq. 34 creating a batch data matrix over the K-samples, we obtain the data equation, that is, defining the matrices as

$$\mathcal{Y}_{\ell,m;K} = \Big[\mathbf{y}_m(\ell) \ \cdots \ \mathbf{y}_m(\ell+K-1)\Big] \tag{35}$$

$$\mathcal{U}_{\ell,m;K} = \Big[\mathbf{u}_m(\ell) \ \cdots \ \mathbf{u}_m(\ell+K-1)\Big] \tag{36}$$

$$\mathcal{X}_{\ell,m;K} = \Big[\mathbf{x}_m(\ell) \ \cdots \ \mathbf{x}_m\ell+K-1)\Big] = \Big[\mathbf{x}(\ell) \ A\mathbf{x}(\ell) \ \cdots \ A^{K-1}\mathbf{x}(\ell)\Big] \tag{37}$$

we obtain the *data equation* that relates the system model to the data (input and output matrices)

$$\mathcal{Y}_{\ell,m;K} = \mathcal{O}_K \mathcal{X}_{\ell,m;K} + \mathcal{T}_K \mathcal{U}_{\ell,m;K} \tag{38}$$

This expression represents the fundamental relationship for the input-state-output of a linear time-invariant (LTI) state-space system that will be exploited next.

3.0 State-Space Identification: Subspace Approach

In this section we develop the basic subspace approach to state-space system identification. We start with the fundamental problem of identifying or extracting the state-space system $\Sigma = \{A, B, C, D\}$—the realization problem and then evolve to the development of subspace identification techniques. First, we investigate the basis of realization methods.

The *realization problem* is simply stated as:

GIVEN a set of impulse response matrices $\{H_i(t)\}$ with corresponding Markov parameters, $H_i = CA^tB + D\delta(t)$; $t = 0, 1, \cdots, K-1$, FIND the corresponding state-space system, $\Sigma := \{A, B, C, D\}$.

The solution to this deterministic problem proceeds by first creating the *Hankel matrix* defined by

$$\mathcal{H}_{m;K} = \begin{bmatrix} H_0 & H_1 & \cdots & H_{K-1} \\ H_1 & H_2 & \cdots & H_K \\ \vdots & \vdots & \vdots & \vdots \\ H_m & H_{m-1} & \cdots & H_{m+K-2} \end{bmatrix} = \begin{bmatrix} CB & CAB & \cdots & CA^{K-1}B \\ CAB & CA^2B & \cdots & CA^KB \\ \vdots & \vdots & \vdots & \vdots \\ CA^{m-1}B & CA^mB & \cdots & CA^{m+K-2} \end{bmatrix} \tag{39}$$

and therefore,

$$\mathcal{H}_{m;K} = \mathcal{O}_m \times \mathcal{C}_K \tag{40}$$

where $\mathcal{O}_m$ is the *observability matrix* defined previously, while $\mathcal{C}_K$ is the *controllability matrix* (reachability matrix) [1] defined by

$$\mathcal{C}_K := \begin{bmatrix} B & AB & \cdots & A^{K-1}B \end{bmatrix} \tag{41}$$

Some important system theoretic properties of Hankel matrices are:

- The system defined by Σ is *minimal* if and only if it is *completely controllable* and *completely observable* [Minimal Order]
- For a minimal realization, Σ the rank of the Hankel matrix satisfies: $\rho[\mathcal{H}_{m,K}] \leq \min\left\{\rho[\mathcal{O}_m], \rho[\mathcal{C}_K]\right\} \leq N_x$ [Rank Property]

- $\rho[\mathcal{H}_{m,K}] = \rho[\mathcal{H}_{m+1,K}] = \rho[\mathcal{H}_{m,K+1}] = N_x$ [Shift Property]

Such a minimal realization is *stable* if:

- The eigenvalues of the system matrix A lie within the unit circle: $\lambda\Big[A\Big] \leq 1$
- The corresponding observability and controllability Gramians defined below satisfy the positivity constraints:

$$\Sigma_{AC} = A^T \Sigma_{AC} A + C^T C \geq 0 \qquad \text{[Observability Gramian]}$$

$$\Sigma_{AB} = A \Sigma_{AB} A^T + B B^T \geq 0 \qquad \text{[Controllability Gramian]}$$

Applying these properties, we define a *balanced realization* for a stable system A matrix as:

- For $\Sigma_{AB} = \Sigma_{AC} = \Sigma_K$ where Σ is a diagonal matrix such that

$$\Sigma_K = \text{diag}\Big[\sigma_1, \sigma_2, \cdots, \sigma_K\Big] \text{ for } \sigma_1 \geq \sigma_2 \geq \cdots \sigma_K$$

  and Σ_K is given by the singular value decomposition (SVD) of the Hankel matrix:

$$\mathcal{H}_{K,K} = \mathcal{U}_K \Sigma_K \mathcal{V}_K$$

- The resulting realization is said to be *scale invariant* [24], that is, the balanced realized is robust to amplitude scaling.

We also note from the shift invariant property of the Hankel matrix (above) that

$$\mathcal{H}^{\uparrow}_{K,K} = \mathcal{O}^{\uparrow}_K \mathcal{C}_K = \mathcal{O}_K A \times \mathcal{C}_K = \mathcal{O}_K \times A\mathcal{C}_K := \mathcal{H}^{\leftarrow}_{K,K} \tag{42}$$

since

$$\mathcal{O}^{\uparrow}_K = \underbrace{\begin{bmatrix} C \\ CA \\ \vdots \\ CA^{K-1} \end{bmatrix}}_{\mathcal{O}_K} \times A = \underbrace{\begin{bmatrix} CA \\ CA^2 \\ \vdots \\ CA^{K} \end{bmatrix}}_{\mathcal{O}^{\uparrow}_K}$$

and

$$\mathcal{C}_K^{\leftarrow} = A \times \underbrace{\begin{bmatrix} B & AB & \cdots & A^{K-1}B \end{bmatrix}}_{\mathcal{C}_K} = \underbrace{\begin{bmatrix} AB & A^2B & \cdots & A^KB \end{bmatrix}}_{\mathcal{C}_K^{\leftarrow}}$$

3.0.1 Deterministic State-Space Realizations

Now we have the basic tools to solve the *deterministic realization problem* by performing the SVD of the Hankel matrix, $\mathcal{H}_{m,K}$ where $m \geq N_x$ and $K \geq N_x$ with N_x the dimension of the minimum realization (system) or equivalently the underlying *true* number of states; therefore,

$$\mathcal{H}_{m,K} = \begin{bmatrix} \mathcal{U}_{N_x} & \mathcal{U}_N \end{bmatrix} \begin{bmatrix} \Sigma_{N_x} & 0 \\ 0 & 0 \end{bmatrix} \begin{bmatrix} \mathcal{V}_{N_x}^T \\ \mathcal{V}_N^T \end{bmatrix} = \mathcal{U}_{N_x} \Sigma_{N_x} \mathcal{V}_{N_x}^T \tag{43}$$

for $\Sigma_{N_x} = \text{diag}\begin{bmatrix} \sigma_1, \sigma_2, \cdots, \sigma_{N_x} \end{bmatrix}$

From the factorization of the Hankel matrix and its SVD, we have that

$$\mathcal{H}_{m,K} = \mathcal{O}_m \times \mathcal{C}_K = \underbrace{\left(\mathcal{U}_{N_x} \Sigma_{N_x}^{1/2}\right)}_{\mathcal{O}_{N_x}} \underbrace{\left(\Sigma_{N_x}^{T/2} \mathcal{V}_{N_x}^T\right)}_{\mathcal{C}_{N_x}} \tag{44}$$

where Σ_{N_x} is the matrix square root, that is, $R = S^{1/2} \times S^{T/2}$ obtained by the Cholesky decomposition [13].

Now from shifting properties (above) of the observability (or controllability) matrix we can obtain the system matrices from either [5], [6], [7]

$$\mathcal{O}_{N_x - 1} \times A = \mathcal{O}_{N_x}^{\uparrow}$$

$$A \times \mathcal{C}_{N_x - 1} = \mathcal{C}_{N_x}^{\leftarrow}$$

which yields the system matrices by applying the pseudo-inverse $\left(Z^{\#} := (Z^T Z)^{-1} Z^T\right)$

$$A = \mathcal{O}_{N_x - 1}^{\#} \times \mathcal{O}_{N_x}^{\uparrow}$$

or

$$A = \mathcal{C}_{N_x}^{\leftarrow} \times \mathcal{C}_{N_x - 1}^{\#}$$

with the input and output matrices extracted directly from the controllability and observability matrices as

$$B = \mathcal{C}(1:N_x, 1:N_u) \;\text{ and }\; C = \mathcal{O}(1:N_y, 1:N_x) \tag{45}$$

where recall the N_u is the dimension of the input vector $\mathbf{u}$ and N_y that of the output or measurement vector $\mathbf{y}$ with the notation (Matlab) $1:N \rightarrow 1, 2, \cdots, N$ or equivalently *select* the corresponding rows (columns) 1-to-N of the matrix.

3.0.2 Stochastic Realization

In this section we briefly develop the innovations model for a discrete-time system which is related to a Gauss-Markov representation and then show how it is a special case of this structure.

The Gauss-Markov model for correlated process and measurement noise is given by

$$\begin{aligned} x(t) &= Ax(t-1) + Bu(t-1) + W(t-1)w^*(t-1) \\ y(t) &= Cx(t) + v^*(t) \end{aligned} \tag{46}$$

where $R^*(t,k) := R^*\delta(t-k)$ and

$$R^* := \left[\begin{array}{c|c} R_{w^*w^*} & R_{w^*v^*} \\ \hline R_{v^*w^*} & R_{v^*v^*} \end{array}\right] = \left[\begin{array}{c|c} WR_{ww}W' & WR_{wv} \\ \hline R_{vw}W' & R_{vv} \end{array}\right]$$

and the $(N_x + N_v) \times (N_x + N_v)$ block covariance matrix, R^*, is full with cross-covariance matrices $R_{w^*v^*}$ on its off-diagonals.

The innovations model is a constrained version of the correlated Gauss-Markov characterization. If we assume that $\{e(t)\}$ is a zero-mean, white, Gaussian sequence, that is $e \sim \mathcal{N}(0, R_{ee})$, then a particular Gauss-Markov model for a time-invariant system evolves defined as the *innovations model* [1] by:

$$\begin{aligned} x(t) &= Ax(t-1) + Bu(t-1) + Ke(t-1) \\ y(t) &= Cx(t) + Du(t) + e(t) \end{aligned} \tag{47}$$

where $e(t)$ is the N_y-dimensional innovations vector and K is the $(N_x \times N_y)$ gain (Kalman) or weighting matrix.

$$R^*_{ee} := \text{cov}\left(\left[\begin{array}{c} Ke(t) \\ e(t) \end{array} \right], \left[\begin{array}{c} Ke(t) \\ e(t) \end{array} \right] \right) = \left[\begin{array}{c|c} KR_{ee}K' & KR_{ee} \\ \hline R_{ee}K' & R_{ee} \end{array} \right] \delta(t-k)$$

Comparing the innovations model to the Gauss-Markov model, we see that they both are equivalent corresponding to the case where w and v are correlated.

We define the *stochastic realization problem* as:

GIVEN a set of input/output data, $\{u(t), y(t)\},\ k = 1, \cdots, N$; **FIND** the "best" (minimum error variance) set of the unknown parameters, $\Sigma_{INV} := \{A, B, C, D, K, R_{ee}, x(0), P(0)\}$ that characterize the innovations model of Eq. 47.

Before we discuss the solution to this problem, let us investigate the properties of the innovations model more closely. In our usual model development, we start with the Gauss-Markov representation given by the model set $\Sigma_{GM} := \{A, B, C, D, R_{ww}, R_{vv}, R_{wv}, x(0), P(0)\}$ and a variety of state-space problems are defined within this framework (e.g. state estimation). The same problems can be defined in terms of this model. Therefore, the model set for the innovations model is defined as $\Sigma_{INV} := \{A, B, C, D, K, R_{ee}, x(0), P(0)\}$. The only problem here is that we are usually "not" usually given, Σ_{INV}, but Σ_{GM}. From the equivalence of these models, it is possible to show that if we are given Σ_{GM} and we want to obtain Σ_{INV}, then we must develop the relations between the parameters of the model sets.

The equivalent solution is given by the set of relations called the *Kalman-Szego-Popov* (*KSP*) equations. The *KSP* equations can be solved iteratively to obtain (K, R_{ee}) by directly implementing the innovations model for the *time invariant* case. It can be shown that corresponding to a spectral factor, we can define a stochastic realization, $\Sigma_{KSP} := \{A, B, C, D\}$ based on the generalized *KSP* lemma by using the equivalence of the spectral factors to the sum decomposition of the state-space power spectral density (see [1] for details). The proof follows by equating like terms in the sum decomposition and spectral factors from the *KSP* lemma. It can also be shown that any stochastic realization given by Σ_{KSP} may not satisfy the *KSP* equations

uniquely; therefore, we turn to the innovations model which does provide a *unique* solution. The *innovations model* for the time-invariant case is given by

$$\begin{aligned} \hat{x}(t) &= A\hat{x}(t-1) + Bu(t-1) + Ke(t-1) \\ y(t) &= C(t)\hat{x}(t) + Du(t) + e(t) \end{aligned} \tag{48}$$

where the innovations is $e \sim \mathcal{N}(0, R_{ee})$, the state (estimate) is $\hat{x}(t)$, K is the optimal $N_x \times N_y$ gain (Kalman) or weighting matrix with corresponding estimated state covariance, $\hat{\mathcal{P}} := \text{Cov}(\hat{x}(t))$.

Equating the decomposition with the factors using the innovations model yields the *KSP* equations where the resulting covariance relations are given by and $\hat{\mathcal{P}}$ is the estimated state covariance,

$$\begin{aligned} \hat{P} - A\hat{P}A' &= KR_{ee}K' \\ B - AC' &= KR_{ee} \\ D + D' - C\hat{P}C' &= R_{ee} \end{aligned} \tag{49}$$

Solving these equations iteratively: $R_{ee}(i) \to R_{ee}$, $K(i) \to K$ and $\hat{\mathcal{P}}(i) \to \mathcal{P}$ yields the *KSP* algorithm using the innovations model summarized in Table 1.

Summarizing the solution to the stochastic realization problem, we must:

- Obtain the state-space realization $\Sigma_{KSP} := \{A, B, C, D\}$ using a subspace identification algorithm and the Hankel matrix populated with covariance rather than impulse response matrices ($\mathbf{R}_{yy}(\ell) := \text{cov}\Big(\mathbf{y}(t)\mathbf{y}(t_{k+\ell}\Big); \ell = 0, 1, \cdots, L$) ([25],[26])
- Iteratively solve the *KSP* equations (Table 1) for the associated gain and innovations covariance (K, R_{ee})

Table 1. KSP Iterative Algorithm:

Innovations Covariance

$$R_{ee}(i) = D + D' - C\hat{\mathcal{P}}(i)C'$$

Gain

$$K(i) = \left(B - A\hat{\mathcal{P}}(i)C'\right) R_{ee}^{-1}(i)$$

Estimated Covariance

$$\hat{\mathcal{P}}(i+1) = A\hat{\mathcal{P}}(i)A' + K(i)R_{ee}(i)K'(i)$$

Initial Conditions

$$\hat{\mathcal{P}}(0)$$

Stopping Rule

$$\left|I - \hat{\mathcal{P}}(i) \times \hat{\mathcal{P}}^{-1}(i+1)\right| \leq \epsilon \quad \text{for} \quad \epsilon << 1$$

This completes the fundamental background information required to comprehend the subsequent techniques developed.

4.0 Subspace Identification

In this section we develop the fundamental subspace approach to extracting the state-space realization from input-output data extending the realization from impulse response data—still assumed *deterministic*. Input-output data can be handled in a fashion similar to the impulse response data just discussed. In this case we must return to the "data matrices" developed previously and create similar structures based on sound system theoretical concepts as before.

Here we assume we are given input-output data corresponding to a LTI system with vector inputs $\mathbf{u} \in \mathcal{R}^{\mathbf{N_u \times 1}}$ and vector outputs $\mathbf{y} \in \mathcal{R}^{\mathbf{N_y \times 1}}$ with discrete time samples, $t = 0, 1, \cdots, K$ such that the input-output data is given respectively by (as before)

$$\mathbf{u} = [\mathbf{u}(0) \;\; \mathbf{u}(1) \;\; \cdots \;\; \mathbf{u}(K-1)]^T \;\text{ and }\; \mathbf{y} = [\mathbf{y}(0) \;\; \mathbf{y}(1) \;\; \cdots \;\; \mathbf{y}(K-1)]^T$$

Suppose we have k-data samples such that $k > N_x$, then the corresponding block Hankel matrices can be created directly from Eq. 35 with the shift k to give both *vector* input-output (state) relations

$$\mathbf{y}_k(t) = \mathcal{O}_k \mathbf{x}(t) + \mathcal{T}_k \mathbf{u}(t) \tag{50}$$

and the corresponding *matrix* input-output (state) equation as

$$\mathcal{Y}_{k|2k-1} = \mathcal{O}_k \mathcal{X}_k + \mathcal{T}_k \mathcal{U}_{k|2k-1} \tag{51}$$

where the matrices are defined (as before) in Eqs. 35-37.

The *initial states* are given by

$$\mathcal{Y}_{0|k-1} = \mathcal{O}_k \mathcal{X}_0 + \mathcal{T}_k \mathcal{U}_{0|k-1} \tag{52}$$

Here $\mathcal{U}_{0|k-1},\ \mathcal{Y}_{0|k-1}$ are the *past* inputs and outputs, while $\mathcal{U}_{k|2k-1},\ \mathcal{Y}_{k|2k-1}$ are the future inputs and outputs which are all *block Hankel* matrices [22]-[26].

Next we define the *augmented* (input-output) *data matrix* $\mathcal{D}$ along with its corresponding LQ-decomposition as:

$$\mathcal{D}_{0|k-1} := \begin{bmatrix} \mathcal{U}_{0|k-1} \\ -- \\ \mathcal{Y}_{0|k-1} \end{bmatrix} = \begin{bmatrix} \mathbf{I} & 0 \\ - & - \\ \mathcal{T} & \mathcal{H} \end{bmatrix} = \begin{bmatrix} \mathbf{I} & 0 \\ - & - \\ \mathcal{T} & \mathcal{O}\mathcal{C} \end{bmatrix} = \begin{bmatrix} \mathbf{L}_{11} & 0 \\ - & - \\ \mathbf{L}_{21} & \mathbf{L}_{22} \end{bmatrix} \times \begin{bmatrix} Q_1^T \\ Q_2^T \end{bmatrix} \tag{53}$$

or simply

$$\mathcal{O}_k \mathcal{X}_0 Q_2 = L_{22} \tag{54}$$

which implies that the rank $\rho(L_{22}) = N_x$.

Therefore, performing the SVD of L_{22}, that is,

$$L_{22} = \begin{bmatrix} \mathcal{U}_1 & \mathcal{U}_2 \end{bmatrix} \begin{bmatrix} \Sigma_1 & 0 \\ 0 & 0 \end{bmatrix} \begin{bmatrix} \mathcal{V}_1^T \\ \mathcal{V}_2^T \end{bmatrix} \tag{55}$$

yields

$$\mathcal{O}_k \mathcal{X}_0 Q_2 = \mathcal{U}_1 \times \Sigma_1 \times \mathcal{V}_1^T = \underbrace{(\mathcal{U}_1 \Sigma_1^{1/2})}_{\mathcal{O}_k} \times \underbrace{(\Sigma_1^{T/2} \mathcal{V}_1^T)}_{\mathcal{C}_k} \tag{56}$$

and as before the system matrices are A, B, C, D can be extracted by:

$$A = \mathcal{O}_{N_x-1}^{\#} \times \mathcal{O}_{N_x}^{\uparrow}; \qquad C = \mathcal{O}(1 : N_y, 1 : N_x) \tag{57}$$

The input transmission an direct feedthrough matrices B and D can be obtained by solving a least-squares problem using the pseudo-inverse $\left(Z^{\#} := (Z^T Z)^{-1} Z^T\right)$ that directly that leads to the following solution

$$\begin{bmatrix} \hat{D} \\ \hat{B} \end{bmatrix} = Z^{\#} Z^T \times (\mathcal{U}_2^T L_{21} L_{11}^{-1}) \tag{58}$$

(see [25], [26] for more details).

We develop the algorithm in more detail in Appendix A. Therefore, we have the **M***ultivariable* **O***utput* **E***rror* **S***tate-S***P***ace* (MOESP) algorithm given by:

- Compute the LQ-decomposition of $\mathcal{D}$ of Eq. 53;
- Perform the SVD of L_{22} in Eq. 55 to extract $\mathcal{O}_k$;
- Obtain A and C from Eq. 57; and
- Solve the least-squares problem to obtain B and D from Eq. 58.
- Solve the *KSP* equations to obtain K and R_{ee} from Eq. 49.

Finally for the *deterministic realization problem* from input-output data, we develop an alternative *oblique* projection method based on the data matrix [25]. This *oblique* projection algorithm is termed **N**umerical algorithms **4** **S**ubspace **ID**entification (N4SID) and is developed in Appendix B.

Following the "road-map" of Fig. 1.0 developed in the introduction, we proceed to the application of the *identified* vibrational model to anomaly detection by employing these "identified" models first in a model-based processing scheme.

5.0 Subspace Approach to Vibrational System Identification

The overall approach to modal-frequency tracking/anomaly detection is based on the development of robust subspace identification techniques that can be applied to solve this problem—in real-time. The main idea is to pre-process a

section or window of digitized data and perform a system (vibrational) identification followed by an extraction of the underlying modes from the identified model producing raw estimates of the corresponding modal frequencies and mode shapes (not discussed here). Once the "raw" modal frequencies in each window are extracted a sequential tracking algorithm (Kalman filter) is applied to "smooth" the estimates which are eventually input to a corresponding change or anomaly detection algorithm (not discussed here) for monitoring performance. This approach is highly dependent on the particular subspace identification algorithm selected as well as the underlying order (2 × number of modes) of the vibrational system under investigation. For instance,a 12-mode (24-state) identification requires a minimum data-window of 3000-samples that is approximately a 3 sec time-window, while a 25-mode (50-state) identification requires a data-window of 7000-samples (9 sec time-window); therefore, a real-time application must take these factors into account when selecting order.

In this section we outline the model-based approach to vibrational system anomaly detection for our problem. The overall objective is to develop a model-based method capable of monitoring of a vibrational system providing operational status (normal), detecting and classifying anomalies (abnormal) in real-time. We summarize the major steps required to achieve this goal in Fig. 2

- *Pre-process* (outliers, whitening, bandpass filtering, normalization) data relative to the targeted vibrational system information.
- *Identify* (subspace) underlying vibrational model from the data sets in state-space form $\Sigma = \{A, B, C, D\}$.
- *Transform* identified model to the modal state-space representation $\Sigma_M = \{A_M, B_M, C_M, D_M\}$.
- *Extract* modal frequencies and mode shapes from the modal state-space model.
- *Track* (Kalman filter) the raw frequencies *sequentially* in real-time.
- *Detect* anomalies using a sequential (real-time) model-based detector.
- OFF-Line

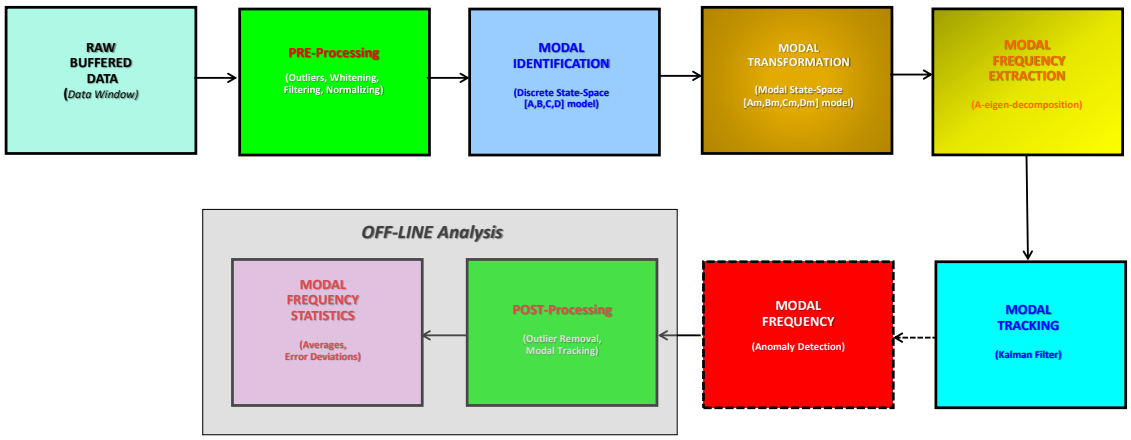

Figure 2: Model-Based Dynamic Monitoring: PRE-processing, modal identification, modal frequency extraction, modal tracking, anomaly detection, POST-processing, performance statistics.

- *Post-process* (outlier/tracker) the on-line tracking data.
- *Estimate* the modal frequency statistics to evaluate performance.

Next we discuss each of these steps in more detail.

5.0.1 Pre-Processing

Pre-processing of the acquired vibrational data is a crucial first step in the signal processing. It is designed to extract the "targeted" frequencies and remove outliers, sample (2.25 × Nyquist frequency) to minimize the rate, enhance or equalize the modal frequencies, filter any disturbances outside the band of interest and normalize the filtered data to scale the data for identification.

Outlier detection/correction is based on the *median absolute deviation* (*MAD*) statistic because of its inherent robustness property relative to the usual mean/standard deviation approach [34], [35]. *MAD* is defined as

$$\mathcal{MAD}(t) := \gamma \; \mathcal{M}_t \left(|Y_t - \mathcal{M}_i(Y_i)| \right) \tag{59}$$

where $Y_t := \{y(0), \cdots, y(t)\}$ is the set of discrete-time data up to time t, $\mathcal{M}_t$ is the median of the data, and $\gamma = 1.4826$ is a constant based on the normalized (assumed Gaussian) data. The outliers are detected using the bounds

$$\mathcal{M}_t - \beta \times \mathcal{MAD}(t) \; < \; Y_t \; < \; \mathcal{M}_t + \beta \times \mathcal{MAD}(t) \tag{60}$$

where β is a threshold equivalent to a confidence limit—we selected $\beta = 4$ for our data sets [34], [35]. Due to the limited amount of estimated modal frequency samples available in our application, we replaced the detected outlier with the median amplitude of the data as shown in Fig. 3 usually less than 1% of the samples/window.

Once the outliers are detected/corrected from each of the measurement channels an equalizing or whitening filter was applied to the data set for each channel. For this implementation we applied a $1-3$ order, all-pole (autoregressive) filter with the coefficients estimated using the Levinson-Durbin recursion (see [1])

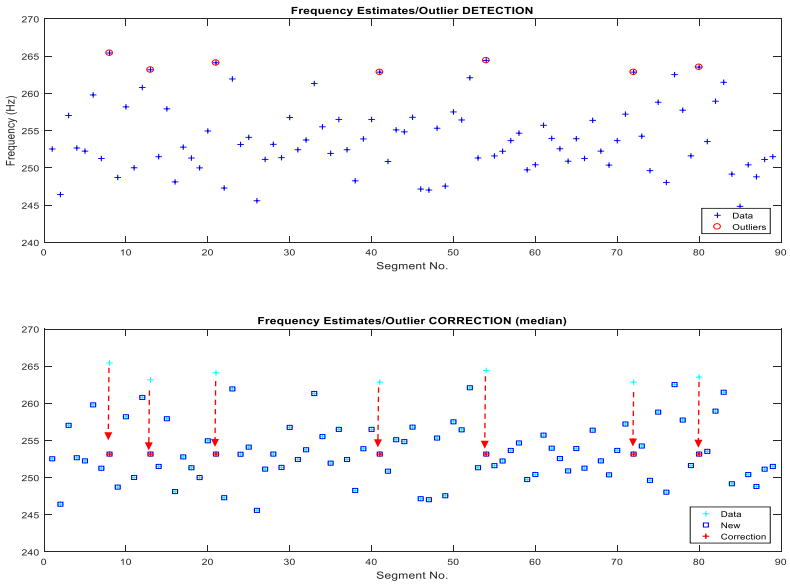

Figure 3: Outlier Detection/Correction: (a) Raw measurement channel data with outlier detection. (b) Measurement channel with outlier correction to the median value.

$$y(t) = -\alpha_1 y(t-1) - \alpha_2 y(t-2) - \alpha_3 y(t-3) + \sigma\epsilon(t);\ t = 1, \cdots, N_t \quad (61)$$

where $\{\alpha_i\}$ is the set of estimated filter coefficients, σ is the filter gain and ϵ is the corresponding error sequence [1]. With the coefficients estimated, an *inverse* filter was applied to the data to achieve the desired results an provide an equalized sequence at each channel $\{\epsilon(t)\}$, that is,

$$\epsilon(t) = -\alpha_1 \epsilon(t-1) - \alpha_2 \epsilon(t-2) - \alpha_3 \epsilon(t-3) + \sigma y(t);\ t = 1, \cdots, N_t \quad (62)$$

With the data corrected and equalized, the resulting channels are then bandpass filtered using a classical, 12-th order, analog prototype, Butterworth digital filter providing a maximally-flat magnitude response between the frequency ranges of $180 - 400$ Hz—our targeted modal frequencies.

$$y_{f_n}(t) = -\sum_{i=1}^{N_f} c_i \epsilon(t-i);\ t = 1, \cdots, N_t \quad (63)$$

where the $\{c_i\}$ are the N_f pre-calculated Butterworth filter coefficients for the n-th channel. We also applied a bandstop filter in the frequency range of $290-320$ Hz, since we know a-priori from the power spectrum of the raw data that a notch is present in the data sets indicating that the structure has no modal frequencies in that region of interest. Finally, this set of filtered channel data $\{y_{f_n}(t)\}$ is *normalized* scaling it to provide multiple input/multiple output data for the subspace identification algorithm such that

$$y_n(t) = \frac{y_{f_n}(t) - \mu_{f_n}}{\sigma_{f_n}};\ n = 1, \cdots, N_y \quad (64)$$

where μ_{f_n} and σ_{f_n} are the corresponding mean and standard deviations of the n-th channel time series. This completes the pre-processing. Next we consider the subspace identification.

5.0.2 Subspace Identification

After pre-processing the window of raw vibration data, the subspace identification algorithm is applied to estimate the discrete-time *MIMO* state-space model, $\hat{\Sigma}(m) = \{\hat{A}(m), \hat{B}(m), \hat{C}(m), \hat{D}(m)\}$ as discussed in Sec. 4.

5.0.3 Transformation to Modal State-Space

With this estimated model, $\hat{\Sigma}(m)$, available after processing the m-th data window, we can now transform the identified discrete-time modal to the modal state space by applying the similarity transformation (T_M) based on the eigen-transformation of $A(m) \rightarrow A_M(m)$ (eigenvalue-eigenvector) as discussed in Sec. 2 enabling the new model set $\hat{\Sigma}_M(m) = \{\hat{A}_M(m), \hat{B}_M(m), \hat{C}_M(m), \hat{D}_M(m)\}$.

5.0.4 Modal Frequency Extraction

Modal frequencies and mode shapes (not discussed here) are now extracted from the transformed model, $\Sigma_M(m)$, by performing the simple discrete-time to continuous-time transformation of the $\mathcal{Z}$-domain to the Fourier domain $\mathcal{F}$, that is, $\sigma(m) \pm 2\pi f(m) \rightarrow \frac{1}{\triangle t} \ln\left(\mathrm{Re}[\mathcal{Z}] \pm \mathrm{Im}[\mathcal{Z}]\right)$ providing the set of modal frequencies for post-processing and tracking, $\{\hat{f}_n(m)\}; 1, \cdots, N_m$ where N_m is the number of modes ($2 \times$ states) selected for the identification.

5.0.5 Modal Frequency Tracking

The modal frequency tracker design is a model-based processor (Kalman filter) that has been applied successfully in wide variety of applications [1], [32], [33]. The underlying frequency estimator/tracker is based on the following Gauss-Markov representation that evolves directly from a finite difference representation of the instantaneous frequency changes.

$$\dot{f}(t) \approx \frac{f(t_{k+1}) - f(t_k)}{\triangle t_k}$$

or re-writing this expression gives

$$f(t_{k+1}) = f(t_k) + \triangle t_k \dot{f}(t_k) \tag{65}$$

Assuming that the frequency change is constant over the sampling interval ($\dot{f}(t_{k+1}) \approx \dot{f}(t_k)$) and the model uncertainty is characterized by Gaussian process noise leads to the following set of discrete-time, Gauss-Markov stochastic equations

$$f(t_{k+1}) \;=\; f(t_k) + \triangle t_k \dot{f}(t_k) + w_1(t_k) \qquad \text{[Frequency]}$$

$$\dot{f}(t_{k+1}) \;=\; \dot{f}(t_k) + w_2(t_k) \qquad \text{[Rate]} \tag{66}$$

where w is zero-mean, Gaussian with $\mathbf{w} \approx \mathcal{N}(0, R_{ww})$. The corresponding measurement is also contaminated with instrumentation noise represented by zero-mean, Gaussian uncertainties as

$$y(t_k) = f(t_k) + v(t_k) \qquad \text{[Measurement]}$$

such that $v \sim \mathcal{N}(0, R_{vv})$. A combination of both process and measurement systems can be placed in a discrete-time ($t_k \rightarrow t$), state-space framework by defining the state vector $x(t) := [f(t) \mid \dot{f}(t)]'$ to give the *Modal-Frequency Gauss-Markov model* as

$$\begin{aligned} x(t+1) &= \begin{bmatrix} 1 & \triangle t \\ 0 & 1 \end{bmatrix} x(t) + w(t) \\ y(t+1) &= [\;1\;\mid\;0\;]x(t+1) + v(t+1) \end{aligned} \tag{67}$$

Now with this underlying frequency model established, we know that the optimal solution to the state estimation or frequency tracking problem is provided by the Kalman filter [1], that is,

$$\hat{x}(t+1|t+1) = \hat{x}(t+1|t) + K(t+1)e(t+1)$$

or in terms of the components (states) we have

$$\begin{aligned} \hat{f}(t+1|t+1) &= \hat{f}(t+1|t) + K_1(t+1)e(t+1) \\ \hat{\dot{f}}(t+1|t+1) &= \hat{\dot{f}}(t+1|t) + K_2(t+1)e(t+1) \\ \hat{y}(t+1|t) &= \hat{f}(t+1|t) \\ e(t+1) &= y(t+1) - \hat{y}(t+1|t) \end{aligned} \tag{68}$$

where $e(t)$ is the innovations/residual sequence and $K(t)$ are the gains or weights. This notation is defined by the conditional mean, $\hat{f}(t+1|t) := E\{f(t+1)|y(t), \cdots, y(0)\}$, that is, the estimate of $f(t+1)$ based on all of the available data up to time t.

Since we are primarily interested in a real-time application, we restrict the processor to reach steady-state, that is, the Kalman gain becomes a constant (steady-state) which can calculated iteratively as in the stochastic realization using the *KSP*-equations or equivalently obtained directly from the discrete Riccati equation to give the frequency tracker relations [1], [32], [33]

$$\begin{aligned} \hat{f}(t+1) &= \hat{f}(t) + K_1 e(t+1) \\ \hat{\dot{f}}(t+1) &= \hat{\dot{f}}(t) + K_2 e(t+1) \\ \hat{y}(t+1) &= \hat{f}(t+1) \\ e(t+1) &= y(t+1) - \hat{y}(t+1) \end{aligned} \tag{69}$$

where K is now a *pre-calculated* constant.

A typical tracking result is shown for a single frequency track in Fig. 4. Note from the raw data that the estimates are contaminated with *correlated* process noise leading to a smoother appearance rather than the usual uncorrelated (white) noise—typical in instrumentation systems. In (a) we see an "optimal" track where the steady-state filter follows the modal frequency variations and provides an enhanced estimate; however, we are interested in applying more smoothing and choose to weight the optimal solution more heavily by multiplying the optimal gain by a fixed scaling constant, that is, $K \rightarrow \mu K$ with μ the scaling constant. The results are shown in Fig. 4b,c where we see that the tracker output provides a much smoother (less variations) for $\mu = 0.1$ and $\mu = 0.01$. It was found after a large number of runs that this approach leads to a very robust tracking solution that is desired for on-line operations.

5.0.6 Post-Processing

After all of the operations have been performed, the subspace approach has essentially evolved from a set of noisy *MIMO* data, to identifying a state-space model at *each* data window and extracting its modal frequencies and shapes. Each of the modal models is available for archiving (if desired) and the resulting set of modal frequencies is available for post-processing. The data that consists of the identified set of modal frequencies and shapes for each of the N_f-frequencies are available for post-processing consisting

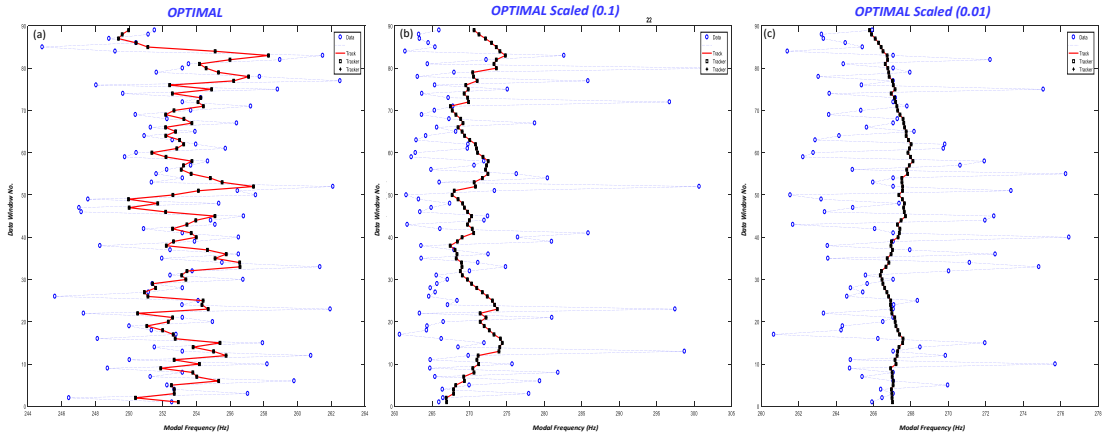

Figure 4: Modal Frequency Tracking for Single Channel: (a) Optimal weighted tracker. (b) Scaled optimal tracker with $\mu = 0.1$. Scaled optimal tracker with $\mu = 0.01$.

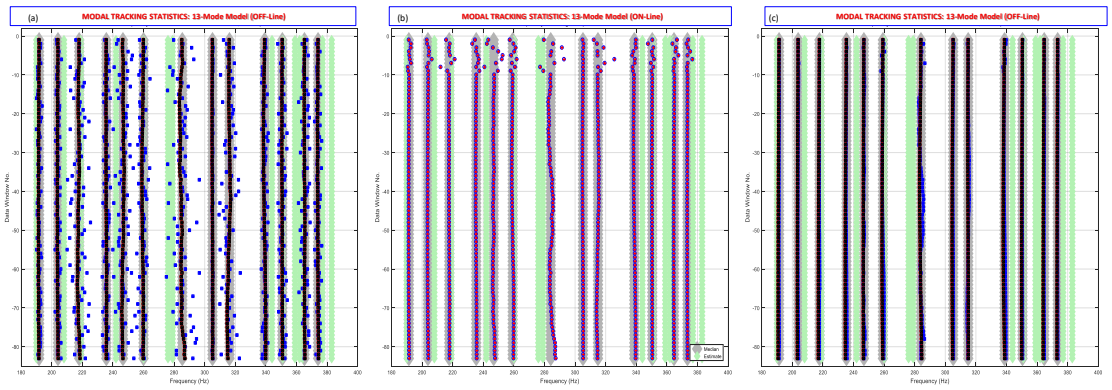

Figure 5: Modal Frequency Tracking using a 13-Mode Model: (a) POST-processed (OFF-line) tracker for raw modal frequencies. (b) ON-line model frequency tracker. (c) POST-processed (OFF-line) tracker for sequential modal frequencies.

of *outlier* detection/correction and further *smoothing* using the frequency tracker (as above). Typical results are shown in Fig. 5 which illustrates the raw modal frequencies directly from the subspace identification in Fig. 5a to the *on-line* estimates of the outlier and tracker in Fig. 5b to the final post-processed modal frequency tracker in Fig. 5c. Here we note the improvement of applying the on-line outlier/tracker combination, initially , and the improved modal frequency estimates after post-processing.

This completes the discussion of the subspace approach, next we apply it to our "unknown" device and evaluate its performance.

6.0 Application: Structural Device

In this section, we discuss the application of the subspace approach to a structurally "unknown" device, that is, a complex, stationary structure (black

-box) with no rotating parts that is subjected to random excitation with accelerometer sensors placed on its surface and around its periphery. We do have some prior information about its modal response from historical tables and use this information as targeted modes (frequencies and shapes) to evaluate the validity and performance of these results as well as guiding any pre-processing of the acquired data.

The device under test was subjected to random excitations by placing a stinger or motor-driven rod perpendicular to the base of the structure. A suite of 19-triaxial accelerometers were positioned strategically about the device surface as well as a single sensor allocated to measure the excitation time series. In total, an array of 57-accelerometer channels acquired a set of 10-minute duration data at a $6.4KHz$ sampling frequency. The data were subsequently down-sampled to $0.9KHz$ in order to focus on the targeted modal frequencies ($< 400Hz$). From the state-space perspective, we have a targeted system of up to a maximum of 14-modes or 28-states with an array of 57 channels of time series measurements and 1-channel of an excitation measurement as illustrated in Fig. 6.

The raw data (down-sampled) represents the expected data acquired from the real-time acquisition system. The long time series were pre-processed by performing outlier detection/correction, whitening filter (optional), bandpass filtering, normalization prior to performing the system identification. Once pre-processed the input/output data were provided to the subspace algorithm that enabled the identification of a discrete-time state-space model, $\Sigma = \{A, B, C, D\}$, that was then transformed to the modal state-space, $\Sigma_M = \{A_M, B_M, C_M, D_M\}$, providing both modal frequencies and mode shape information, that is, modal eigenvalues and eigenvectors. Outliers were detected/corrected from these raw modal frequency estimates and provided as input to the frequency tracker (steady-state Kalman filter [1]) enabling a "smoothed" sequential estimate in real-time. After the data set is processed, modal frequencies and mode shapes extracted, the data are then post-processed to improve the estimates even further by applying a "batch" tracker (Kalman filter) with the improved ensemble statistics, since the entire track of data is now available. These results are then analyzed and provided for eventual anomaly detection (see Fig. 2).

With all of this information available, we first performed a suite of subspace identifications by specifying the number of modes ranging from $9 - 16$,

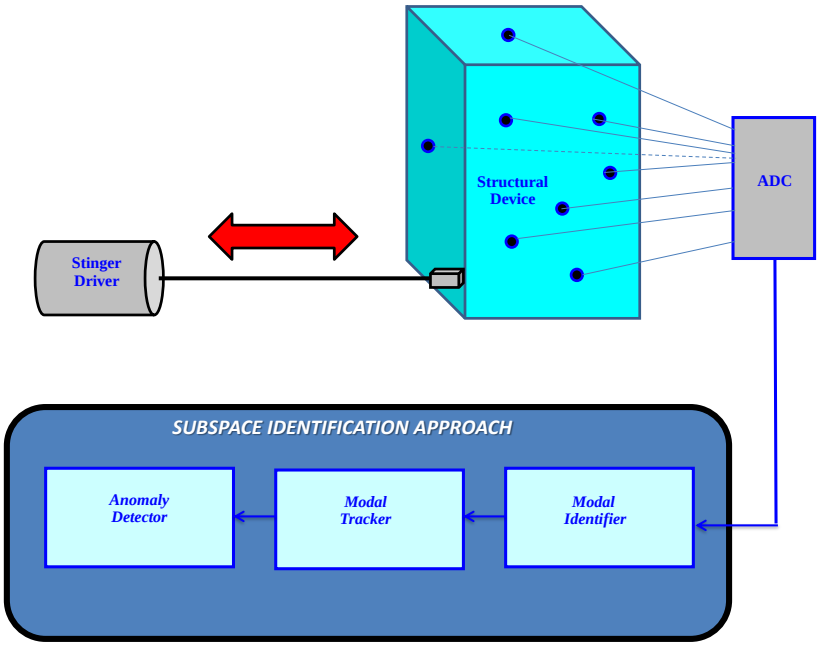

Figure 6: Structural Device Experimental Setup: Motor driven stinger random vibrations, MIMO ADC measurements, subspace identification: identifier, tracker, detector system.

AND 20, 25, with our targeted number was 14 modal frequencies from the historical tables. For each number of these modes, we generated the corresponding frequency tracks one for each modal frequency as shown in Fig. 7 for a 13-mode (26-state) identification. Here we observe the estimated power spectrum of the identified model for each data window in (a) along with the identified modal frequencies (+) in order to illustrate any clustering. In Fig. 7b we see the resulting on-line outlier corrected/tracks for each of the identified modal frequencies. Therefore, an ensemble of frequency estimates resulted for each track for post-processing statistical analysis. Comparisons of the ensemble averages of the identified modal frequencies are shown in Table 2. When the number of modes selected was less than or equal to 14, the tracks were reasonable stable, but only $10-11$ of the target frequencies were essentially captured (within reasonable bounds) by the subspace identifier. Increasing the order greater than 14 enabled another of the targeted modes to be identified ($11 \rightarrow 12$), but found excdessive "false" modes with wild frequency tracks. It is clear from the table that orders less than 12 are not capable of reasonably estimating 10 or more modes and that those orders of 12 and above can capture at least 10 modes.

These frequencies along with their accompanying statistics are used to determine which of the model orders selected enable a "reasonable" estimate of the targeted frequencies as shown in Table 2. Next we are able to select the model order based on the calculated 1 σ standard deviations along with the corresponding percentage relative error[1] statistics. The average results, standard deviations and error percentages, are also shown in the table. Even though the 15 and 16 modal identifications provided somewhat superior statistical estimates of the modal frequencies and the fact that an additional targeted mode was identified, their erratic behavior of the extraneous modes caused concern for eventual on-line failure detection therefore, they were not considered viable candidates. Based on these concerns, we selected the 13-mode (26-state) model for our subspace algorithm providing not only the most reasonable trade-off of deviation/error as well as a practical window time (3300-samples) of 7.1-seconds/identification which is based on the required number of samples for the identification algorithm (ID time x sampling interval). This time is quite reasonable for a 900 Hz sampling frequency and vibrational monitoring of the system. Note that the higher the order, the

[1]Percentage relative error ($\%\epsilon$) is given by $\frac{\text{True}-\text{Estimate}}{\text{True}} \times 100$.

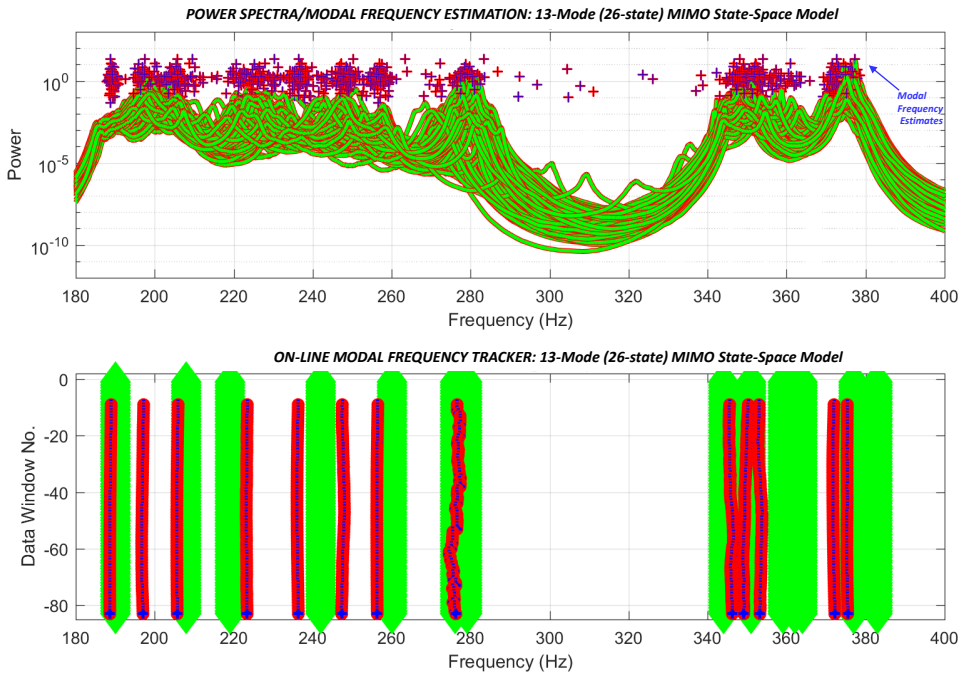

Figure 7: Subspace Identification of 13 Mode Model: (a) Estimated transfer functions of identified modal models and raw modal frequency estimates (+). (b) Sequential (ON-line) modal frequency tracker results with outlier corrections (10-sample initialization).

number of samples for subspace identification increases.

Post-processing of the tracking frequencies were shown in Fig. 5. Clearly, as expected, the *batch* post-processor performing both outlier correction and tracker smoothing, is superior to the on-line tracks primarily because the ensemble statistics of 83 data windows are now available to improve the estimates as illustrated previously in Fig. 5c. The ensemble statistics for the 13-mode identification are shown in Fig. 8 where we see the corresponding scatter plot along with the corresponding 99.9% confidence interval about the mean modal frequency. Clearly the estimates are reasonably precise as shown in (a) and in Table 2 as well. In Fig. 8(b) we observe the corresponding modal frequency histogram with most of the identified frequency bins heavily populated indicating very high probabilities of the modal frequencies estimated by the subspace tracker.

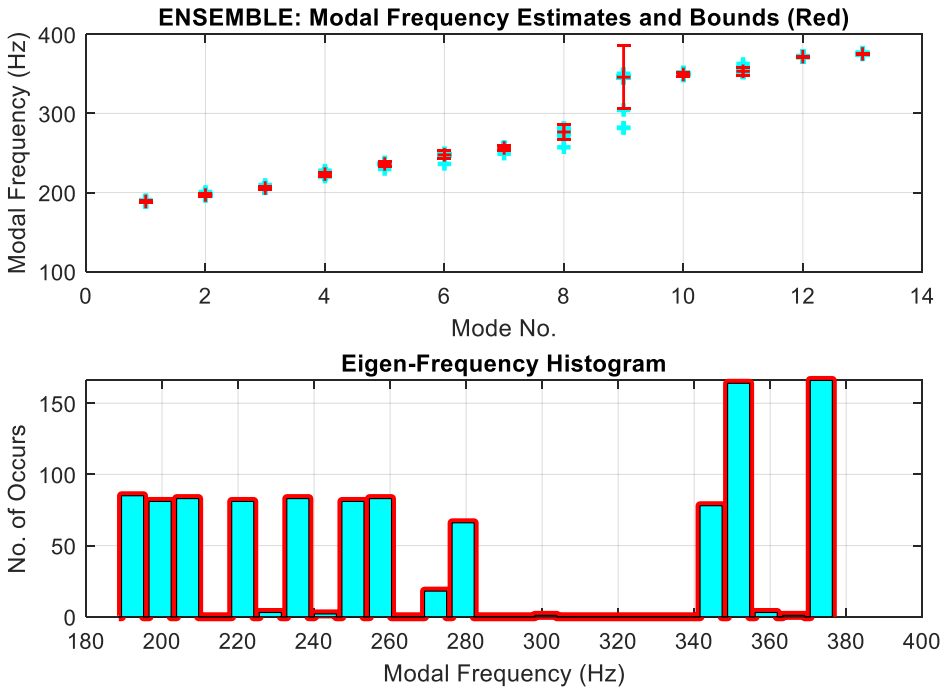

Figure 8: POST-Processing Modal Frequency Tracking Ensemble Statistics: (a) Modal frequency scatter plot with 99.9% confidence limits about the mean. (b) Modal frequency histogram indicating high probabilities in identified modal frequency bins.

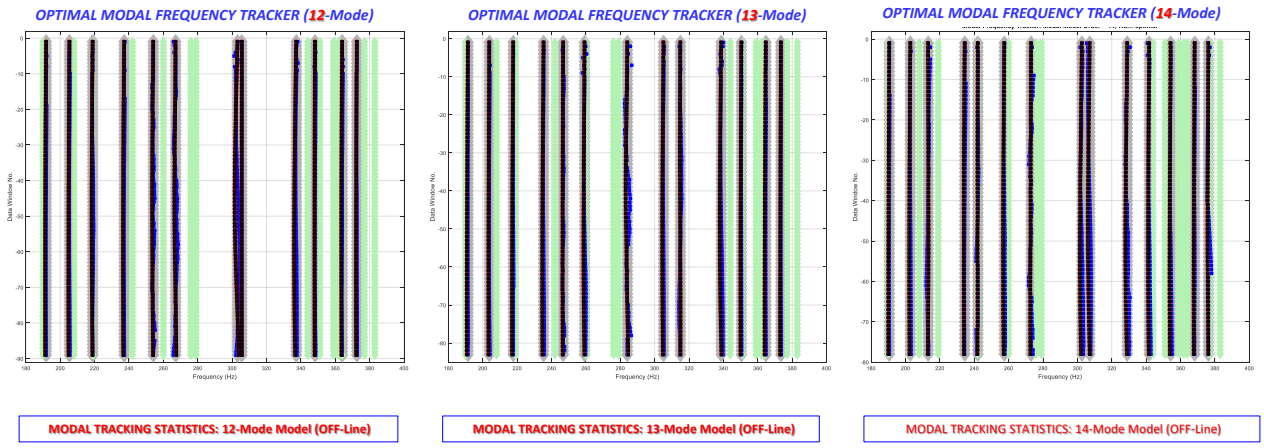

Figure 9: POST-Processed Modal Frequency Tracking of 12-Mode, 13-Mode, 14-Mode Identified State-Space Model Results.

Table 2. MODAL IDENTIFICATION ENSEMBLE STATISTICS

MODAL Frequency Estimates (Relative Error(ϵ))					
Frequency	**12** $\pm\ \sigma(\%\epsilon)$	**13** $\pm\ \sigma(\%\epsilon)$	**14** $\pm\ \sigma(\%\epsilon)$	**15** $\pm\ \sigma(\%\epsilon)$	**16** $\pm\ \sigma(\%\epsilon)$
190 Hz	189±0.2(0.5)	189±0.2(0.5)	189±0.1(0.5)	188±0.2(1.1)	188±0.1(1.1)
208 Hz	207±0.4(0.5)	206±0.5(1.0)	205±0.4(1.4)	204±0.5(1.9)	203±0.4(2.4)
219 Hz	229±2.3(4.6)	223±0.7(0.5)	221±1.2(0.9)	216±0.8(1.4)	213±0.5(2.7)
242 Hz	238±0.8(1.7)	236±0.8(2.1)	241±1.7(0.4)	247±1.0(2.1)	243±0.7(0.4)
260 Hz	260±2.1(0.0)	256±0.8(0.4)	258±3.5(0.8)	254±0.9(2.3)	259±1.1(0.4)
276 Hz	-	276±2.6(0.0)	-	268±3.1(2.9)	276±2.1(0.0)
279 Hz	281±6.3(0.7)	-	279±5.1(0.0)	284±3.8(1.8)	-
344 Hz	347±0.7(0.9)	344±10.8(0.0)	346±7.6(0.6)	348±1.7(1.2)	349±1.4(1.5)
351 Hz	353±0.6(0.6)	350±0.6(0.3)	352±0.6(0.6)	353±0.6(0.6)	354±0.8(0.3)
359 Hz	-	354±1.4(1.4)	359±1.9(0.0)	359±1.9(0.0)	359±1.1(0.0)
362 Hz	-	-	-	-	362±0.9(0.0)
364 Hz	371±0.3(0.0)	372±0.2(2.4)	372±0.4(2.2)	373±0.1(2.5)	373±0.1(2.5)
377 Hz	376±0.3(0.3)	375±0.3(0.5)	377±9.2(0.0)	376±0.3(0.3)	378±0.4(0.3)
383 Hz	-	-	-	-	-
Avg $\sigma(\%\epsilon)$	±1.4 (0.98%)	±1.8 (0.83%)	±3.00 (0.67%)	±1.24 (1.55%)	±0.8 (0.97%)

7.0 Summary

This report summarizes the development of a model-based modal tracking scheme capable of the on-line processing of structural responses applying both system identification methods to extract a modal model and state estimation techniques to track the modal frequencies for eventual anomaly detection and fault location.

Background information on state-space vibrational systems was developed in Sec. 2.0 evolving directly to a multiple input/multiple output (MIMO) structural formulation. From this representation the *modal state-space* model was introduced through an eigenvalue-eigenvector formulation leading to the required similarity transformation and complex modes. Next the sampled-data state-space system eas briefly developed and evolved to a discrete state-space system that provided the basis for the system identification methods to follow. Powerful *MIMO subspace identification* methods were discussed leading to the extraction of a modal state-space model from noisy vibrational measurements. This model provides the essential data required as input to the model-based tracking scheme.

The model-based identifier/tracker was applied to evaluate test data evolving from a vibrating system consisting of approximately 12-modes with 19-directional (X,Y,Z) accelerometer measurements for a total of 57-channels of noisy data. Each of the steps in developing the approach from pre-processing the raw data to subspace identification to model-based tracking were discussed in detail leading to the performance analysis of the tracking techniques completing this effort.

Future work will consist of the development of more robust techniques for real-time operations.

8.0 Acknowledgments

This work performed under the auspices of the U.S. Department of Energy by Lawrence Livermore National Laboratory under Contract DE-AC52-07NA27344.

References

[1] J. V. Candy, *Model-Based Signal Processing*. Hoboken, N.J.:Wiley/IEEE Press, 2006.

[2] L. J. Ljung, *System Identification: Theory for the User*. Englewood Cliffs, N.J.:Prentice-Hall, 1987.

[3] M. R. Hatch, *Vibration Simulation Using MATLAB and ANSYS*. Boca Raton,FL.:Chapman and Hall/CRC Press, 2001.

[4] W. K. Gawronski, *Advanced Structural Dynamics and Active Control of Structures*. London, U.K.:Springer, 2004.

[5] T. Kailath, *Linear Systems*, Upper Saddle River, N.J.:Prentice Prentice Hall, 1980.

[6] J. G. Reid, *Linear System Fundamentals: Continuous, and Discrete, Classic and Modern*, New York, N.Y.:McGraw-Hill, 1983.

[7] R. A. DeCarlo, *Linear Systems: A State Variable Approach with Numerical Implementation*, Engelwood Cliffs, N.J.:Prentice- Hall, 1989.

[8] D. B. McCallen, "Ground Motion Estimation and Nonlinear Seismic Analysis," *Lawrence Livermore National Laboratory Report* **UCRL-JC-121667**, 1995.

[9] D. B. McCallen and A. Astaneh-Asl, "Computational Simulation of the Nonlinear Response of Suspension Bridges," *Lawrence Livermore National Laboratory Report* **UCRL-JC-128901**, 1997.

[10] J. V. Candy and R. B. Rozsa, "Safeguards design for a plutonium nitrate concentrator–an applied estimation approach." *Automatica*, **16**, 1980.

[11] J. V. Candy and E. J. Sullivan, "Ocean acoustic signal processing: a A model-based approach," *J. Acoust Soc. Am.*,vol. 92, no 6, 3185-3201, 1992.

[12] V. Wowk, *Machinery Vibration: Measurement and Analysis*. (New York:McGraw-Hill, 1991).

[13] G. H. Golub and C. F. Van Loan, *Matrix Computations*, 2^{nd} Ed., Baltimore, MD.:The Johns Hopkins University Press, 1989.

[14] H. Van Trees, *Detection, Estimation and Modulation Theory, Pt. 1*, (John Wiley, New York, NY, 1968).

[15] D. F. Specht, "Probabilistic Neural Networks," *Neural Networks*, Vol. 3, 1990.

[16] A. Papoulis and S. Pillai, *Probability, Random Variables and Stochastic Processes*, 4th ed., New York, New York: McGraw-Hill, 2002.

[17] A. Wald, "Sequential tests of statistical hypothesis," *Ann. Math. Stat.*, **16**, pp. 117-186, 1945.

[18] A. Wald, *Sequential Analysis*, New York, N.Y.: John Wiley, 1947 (Reprint Dover Publications, 1973).

[19] A. Willsky, "A survey of design methods for anomaly detection in dynamic systems," Automatica, Vol. **12**, pp. 601-611, (1976).

[20] R. Mehra and J. Peshon, "An innovations approach to fault detection and diagnosis in dynamical systems," Automatica, Vol. 7, pp. 637-640, (1971).

[21] S. G. Azevedo, J. V. Candy and D. L. Lager, "On-line anomaly detection of vibrating structures," Proc. ASME Conf. on Mechanical Vibrations and Noise, Hartford, CT, (1980).

[22] M. Aoki, *State Space Modeling of Time Series*. 2^{nd} Ed., London, U.K.:Springer-Verlag, 1990.

[23] J. Juang, *Applied System Identification*. Upper Saddle River, N.J.:Prentice-Hall PTR, 1994.

[24] P. van Overschee and B. De Moor, *Subspace Idenification for Linear Systems: Theory, Implementation, Applications*. Boston, MA:Kluwer Academic Publishers, 1996.

[25] T. Katayama, *Subspace Methods for System Identification*. London, U.K.:Springer, 2005.

[26] M. Verhaegen and V. Verdult, *Filtering and System Identification: A least-Squares Approach*. Cambridge, U.K.:Cambridge University Press, 2007.

[27] E. Reynders, "System identification methods for (operational) modal analysis: review and comparison," *Archives of Comp. Mehtods Engr.*, Vol. 19 (1), pp. 51-124, 2012.

[28] E. Reynders, J. Houbrechts and G. De Roeck, "Fully automated (oerational) modal analysis," *Mech. Sys. and Signal Proc.*, Vol. 29, pp. 228-250, 2012.

[29] V. Yaghoubi and T. Abrahamson, "The modal observability correlation as a modal correlation metric," *Topics in Modal Anal.*, vol. 7: Proc. of 31 IMAC A Confr., 2013.

[30] J. V. Candy, *Bayesian Signal Processing: Classical, Modern and Particle Filtering Methods*. 2^{nd} Ed., Hoboken, N.J.:Wiley/IEEE Press, 2016.

[31] J. V. Candy, *Signal Processing: The Modern Approach*, New York, N.Y.:McGraw-Hill, 1988.

[32] P. R. Kalata, "The tracking index: a generalized parameter for $\alpha - \beta$ and $\alpha - \beta - \gamma$ target trackers," *IEEE Trans. Aero. and Electron. Sys.*, vol. AES-20, No. 2, pp. 174-182, 1984.

[33] J. H. Painter, D. Kerstetter and S. Jowers, "Reconciling steady-state Kalman and Alpha-Beta filter design," *IEEE Trans. Aero. and Electron. Sys.*, vol. 26, No. 6, pp. 986-991, 1990.

[34] T. Pham-Gia and T. L. Hung, "The mean and median absolute deviations," *Math. Comput. Modeling*, vol. 34, pp. 921-936, 2001.

[35] C. Leys, C. Ley, O. Klein, P. Bernard and L. Licata, "Detecting outliers: Do not use the standard deviation around the mean, use absolute deviation around the median," *J. Exper. Social Psych.*, vol. 49, pp. 764-766, 2013.

A APPENDIX: Subspace Identification—Orthogonal Projections

In this section we develop the fundamental subspace approach to extracting the state-space realization from input-output data extending the realization from impulse response data—still assumed *deterministic*. Input-output data can be handled in a fashion similar to the impulse response data just discussed. In this case we must return to the "data matrices" developed previously and create similar structures based on sound system theoretical concepts as before.

Here we assume we are given input-output data corresponding to a LTI system with vector inputs $\mathbf{u} \in \mathcal{R}^{\mathbf{N_u \times 1}}$ and vector outputs $\mathbf{y} \in \mathcal{R}^{\mathbf{N_y \times 1}}$ with discrete time samples, $t = 0, 1, \cdots, K$ such that the input-output data is given respectively by (as before)

$$\mathbf{u} = [\mathbf{u}(0) \;\; \mathbf{u}(1) \;\; \cdots \;\; \mathbf{u}(K-1)]^T \;\text{ and }\; \mathbf{y} = [\mathbf{y}(0) \;\; \mathbf{y}(1) \;\; \cdots \;\; \mathbf{y}(K-1)]^T$$

Suppose we have k-data samples such that $k > N_x$, then the corresponding block Hankel matrices can be created directly from Eq. 34 with the shift k to give both *vector* input-output (state) relations

$$\mathbf{y}_k(t) = \mathcal{O}_k \mathbf{x}(t) + \mathcal{T}_k \mathbf{u}(t) \tag{70}$$

and the corresponding *matrix* input-output (state) equation as

$$\mathcal{Y}_{k|2k-1} = \mathcal{O}_k \mathcal{X}_k + \mathcal{T}_k \mathcal{U}_{k|2k-1} \tag{71}$$

where the matrices are defined (as before)

$$\begin{aligned}
\mathcal{U}_{k|2k-1} &= \begin{bmatrix} \mathbf{u}_k(t) & \mathbf{u}_k(t+1) & \cdots & \mathbf{u}_k(t+K-1) \end{bmatrix} \\
\mathcal{Y}_{k|2k-1} &= \begin{bmatrix} \mathbf{y}_k(t) & \mathbf{u}_k(t+1) & \cdots & \mathbf{y}_k(t+K-1) \end{bmatrix} \\
\mathcal{X}_k &= \begin{bmatrix} \mathbf{x}(t) & \mathbf{x}(t+1) & \cdots & \mathbf{x}(t+K-1) \end{bmatrix}
\end{aligned}$$

with the *initial states* given by

$$\mathcal{Y}_{0|k-1} = \mathcal{O}_k \mathcal{X}_0 + \mathcal{T}_k \mathcal{U}_{0|k-1} \tag{72}$$

Here $\mathcal{U}_{0|k-1},\ \mathcal{Y}_{0|k-1}$ are the *past* inputs and outputs, while $\mathcal{U}_{k|2k-1},\ \mathcal{Y}_{k|2k-1}$ are the future inputs and outputs which are all *block Hankel* matrices [22]-[26].

Next we define the *augmented* (input-output) *data matrix* $\mathcal{D}$ along with its corresponding LQ-decomposition as:

$$\mathcal{D}_{0|k-1} := \begin{bmatrix} \mathcal{U}_{0|k-1} \\ -- \\ \mathcal{Y}_{0|k-1} \end{bmatrix} = \begin{bmatrix} \mathbf{I} & 0 \\ - & - \\ \mathcal{T} & \mathcal{H} \end{bmatrix} = \begin{bmatrix} \mathbf{I} & 0 \\ - & - \\ \mathcal{T} & \mathcal{OC} \end{bmatrix} = \begin{bmatrix} \mathbf{L}_{11} & 0 \\ - & - \\ \mathbf{L}_{21} & \mathbf{L}_{22} \end{bmatrix} \times \begin{bmatrix} Q_1^T \\ Q_2^T \end{bmatrix} \tag{73}$$

or multiplying the terms and identifying the relations, we have

$$\begin{aligned} \mathcal{U}_{0|k-1} &= L_{11} Q_1^T \\ \mathcal{Y}_{0|k-1} &= L_{21} Q_1^T + L_{22} Q_2^T \end{aligned} \tag{74}$$

or solving for Q_1 and substituting, we have

$$\begin{aligned} Q_1^T &= L_{11}^{-1} \times \mathcal{U}_{0|k-1} \\ \mathcal{Y}_{0|k-1} &= \underbrace{L_{21} L_{11}^{-1} \times \mathcal{U}_{0|k-1}}_{E\{\mathcal{Y}_{0|k-1}|\mathcal{U}_{0|k-1}\}} + \underbrace{L_{22} Q_2^T}_{E\{\mathcal{U}_{0|k-1}|\mathcal{U}_{0|k-1}^{\perp}\}} \end{aligned} \tag{75}$$

These expressions enable the orthogonal decomposition of $\mathcal{Y}_{0|k-1}$; therefore, it follows from Eq. 73 that

$$\mathcal{Y}_{0|k-1} = \mathcal{O}_k \mathcal{X}_0 + \mathcal{T}_k \mathcal{U}_{0|k-1} = \mathcal{O}_k \mathcal{X}_0 + \mathcal{T}_k (L_{11} Q_1^T) = L_{21} Q_1^T + L_{22} Q_2^T \tag{76}$$

but post-multiplying this expression by Q_2 with the ortho-normality/orthogonality conditions of the LQ-decomposition imposed as: $Q_2^T \times Q_2 = I$ and $Q_1^T \times Q_2 = 0$ gives

$$\mathcal{Y}_{0|k-1} Q_2 = \mathcal{O}_k \mathcal{X}_0 Q_2 + \mathcal{T}_k L_{11} \underbrace{Q_1^T Q_2}_{0} = L_{21} \underbrace{Q_1^T Q_2}_{0} + L_{22} \underbrace{Q_2^T Q_2}_{I}$$

or simply

$$\mathcal{O}_k \mathcal{X}_0 Q_2 = L_{22} \tag{77}$$

which implies that the rank $\rho(L_{22}) = N_x$.

Therefore, performing the SVD of L_{22}, that is,

$$L_{22} = \begin{bmatrix} \mathcal{U}_1 & \mathcal{U}_2 \end{bmatrix} \begin{bmatrix} \Sigma_1 & 0 \\ 0 & 0 \end{bmatrix} \begin{bmatrix} \mathcal{V}_1^T \\ \mathcal{V}_2^T \end{bmatrix} \tag{78}$$

yields

$$\mathcal{O}_k\mathcal{X}_0Q_2 = \mathcal{U}_1 \times \Sigma_1 \times \mathcal{V}_1^T = \underbrace{(\mathcal{U}_1\Sigma_1^{1/2})}_{\mathcal{O}_k} \times \underbrace{(\Sigma_1^{T/2}\mathcal{V}_1^T)}_{\mathcal{C}_k} \tag{79}$$

and as before the system matrices are A, B, C, D can be extracted by:

$$A = \mathcal{O}_{N_x-1}^{\#} \times \mathcal{O}_{N_x}^{\uparrow}; \qquad C = \mathcal{O}(1:N_y, 1:N_x) \tag{80}$$

with B and D obtained by solving a least-squares problem directly, since pre-multiplying Eq. 76 by $\mathcal{U}_2^T$ gives

$$\mathcal{U}_2^T\mathcal{O}_k\mathcal{X}_0 + \mathcal{U}_2^T\mathcal{T}_k\mathcal{U}_{0|k-1} = \mathcal{U}_2^TL_{21}Q_1^T + \mathcal{U}_2^TL_{22}Q_2^T$$

but after substituting for $\mathcal{U}_{0|k-1}$ and applying the orthogonality conditions $\mathcal{U}_2^T\mathcal{O}_k = 0$ and $\mathcal{U}_2^TL_{22} = 0$, we have

$$\mathcal{U}_2^T\mathcal{T}_k(L_{11}Q_1^T) = \mathcal{U}_2^TL_{21}Q_1^T$$

post-multiply by Q_1 and using its orthonormal property ($Q_1^TQ_1 = I$) gives

$$\mathcal{U}_2^T\mathcal{T}_k = \mathcal{U}_2^TL_{21} \times L_{11}^{-1} \tag{81}$$

which leads to the least-squares solution

$$\begin{bmatrix} \hat{D} \\ \hat{B} \end{bmatrix} = Z^{\#}Z^T \times (\mathcal{U}_2^TL_{21}L_{11}^{-1}) \tag{82}$$

(see [25], [26] for more details). Therefore, we have the **M***ultivariable* **O***utput* **E***rror* **S***tate-S*P*ace* (MOESP) algorithm given by:

- Compute the LQ-decomposition of $\mathcal{D}$ of Eq. 73;
- Perform the SVD of L_{22} in Eq. 78 to extract $\mathcal{O}_k$;
- Obtain A and C from Eq. 80; and
- Solve the least-squares problem to obtain B and D from Eq. 82.

A APPENDIX: Subspace Identification—Oblique Projections

Finally for the *deterministic realization problem* from input-output data, we develop an alternative *oblique* projection method based on the data matrix [25] by defining first the "past" and "future" operators as:

$$\begin{aligned} \mathcal{U}_p &:= \mathcal{U}_{0|k-1}; \quad \mathcal{Y}_p := \mathcal{Y}_{0|k-1}; \quad \mathcal{X}_p := \mathcal{X}_0 \\ \mathcal{U}_f &:= \mathcal{U}_{k|2k-1}; \quad \mathcal{Y}_f := \mathcal{Y}_{k|2k-1}; \quad \mathcal{X}_f := \mathcal{X}_k \end{aligned}$$

with the matrix input-output relations given by

$$\begin{aligned} \mathcal{Y}_p &= \mathcal{O}_k \mathcal{X}_p + \mathcal{T}_k \mathcal{U}_p \qquad \text{[Past]} \\ \mathcal{Y}_f &= \mathcal{O}_k \mathcal{X}_f + \mathcal{T}_k \mathcal{U}_f \qquad \text{[Future]} \end{aligned} \tag{83}$$

with data matrices, past and future, defined by:

$$\mathcal{D}_p = \begin{bmatrix} \mathcal{U}_p \\ --- \\ \mathcal{Y}_p \end{bmatrix} = \begin{bmatrix} \mathcal{U}_{0|k-1} \\ --- \\ \mathcal{Y}_{0|k-1} \end{bmatrix}; \mathcal{D}_f = \begin{bmatrix} \mathcal{U}_f \\ --- \\ \mathcal{Y}_f \end{bmatrix} = \begin{bmatrix} \mathcal{U}_{k|2k-1} \\ --- \\ \mathcal{Y}_{k|2k-1} \end{bmatrix} \tag{84}$$

The state vector is a basis of the *intersection* of the past and future subspaces and it can be computed by the SVD. First, performing the LQ-decomposition of the past and future data matrices, we have that

$$\begin{bmatrix} \mathcal{U}_f \\ \mathcal{U}_p \\ \mathcal{Y}_p \\ \mathcal{Y}_f \end{bmatrix} = \begin{bmatrix} L_{11} & 0 & 0 & 0 \\ L_{21} & L_{22} & 0 & 0 \\ L_{31} & L_{32} & L_{33} & 0 \\ L_{41} & L_{42} & L_{43} & L_{44} \end{bmatrix} = \begin{bmatrix} Q_1^T \\ Q_2^T \\ Q_3^T \\ Q_4^T \end{bmatrix}$$

which can be rewritten as:

$$\begin{bmatrix} \mathcal{U}_f \\ \mathcal{D}_p \\ \mathcal{Y}_f \end{bmatrix} = \begin{bmatrix} R_{11} & 0 & 0 \\ R_{21} & R_{22} & 0 \\ R_{31} & R_{32} & 0 \end{bmatrix} = \begin{bmatrix} \tilde{Q}_1^T \\ \tilde{Q}_2^T \\ \tilde{Q}_3^T \end{bmatrix} \tag{85}$$

which then leads us to the oblique projection of $\mathcal{Y}_f$ onto $\mathcal{D}_p$ along $\mathcal{U}_f$ [25], [26], that is,

$$\xi := E_{||\mathcal{U}_p}\{\mathcal{Y}_p|\mathcal{D}_p\} = \begin{bmatrix} R_{11} & 0 & 0 \\ R_{21} & R_{22} & 0 \\ R_{31} & R_{32} & 0 \end{bmatrix} = \begin{bmatrix} \tilde{Q}_1^T \\ \tilde{Q}_2^T \\ \tilde{Q}_3^T \end{bmatrix} \tag{86}$$

Decomposing ξ using the SVD, we obtain

$$\xi = \begin{bmatrix} \mathcal{U}_1 & \mathcal{U}_2 \end{bmatrix} \begin{bmatrix} \Sigma_1 & 0 \\ 0 & 0 \end{bmatrix} \begin{bmatrix} \mathcal{V}_1^T \\ \mathcal{V}_2^T \end{bmatrix} = \mathcal{U}_1 \Sigma_1 \mathcal{V}_1^T \tag{87}$$

and therefore equating terms, we have

$$\begin{aligned} \xi = \mathcal{O}_k \mathcal{X}_f &= R_{32} R_{22}^{\#} \mathcal{D}_p \\ \mathcal{O}_k &= \mathcal{U}_1 \Sigma_1^{1/2} \\ \mathcal{X}_f &= \Sigma_1^{1/2} \mathcal{V}_1^T \end{aligned} \tag{88}$$

This *oblique* projection algorithm is termed **N**umerical algorithms **4 S**ubspace **ID**entification (N4SID) [25] and can be summarized by the following steps:

- Compute the LQ-decomposition of ξ of Eq. 87;
- Perform the SVD of ξ in Eq. 88 to extract $\mathcal{O}_k$;
- Compute $\mathcal{X}_f$ of Eq. 88 and define (construct)

$$\begin{aligned} \overline{\mathcal{X}}_{k+1} &= [x(k+1) \ \cdots \ x(k+K-1)] \\ \overline{\mathcal{X}}_{k} &= [x(k) \ \cdots \ x(k+K-2)] \\ \overline{\mathcal{Y}}_{k|k} &= [y(k) \ \cdots \ y(k+K-2)] \\ \overline{\mathcal{U}}_{k|k} &= [u(k) \ \cdots \ u(k+K-2)] \end{aligned}$$

- Obtain A, B, C, D by solving the least-squares problem as:

$$\begin{bmatrix} \overline{\mathcal{X}}_{k+1} \\ --- \\ \overline{\mathcal{Y}}_{k|k} \end{bmatrix} = \begin{bmatrix} A & B \\ C & D \end{bmatrix} \begin{bmatrix} \overline{\mathcal{X}}_{k} \\ --- \\ \overline{\mathcal{U}}_{k|k} \end{bmatrix}$$

$$\begin{bmatrix} \hat{A} & \hat{B} \\ \hat{C} & \hat{D} \end{bmatrix} = \left(\begin{bmatrix} \overline{\mathcal{X}}_{k+1} \\ --- \\ \overline{\mathcal{Y}}_{k|k} \end{bmatrix} \begin{bmatrix} \overline{\mathcal{X}}_{k} \\ --- \\ \overline{\mathcal{U}}_{k|k} \end{bmatrix}^T \right) \left(\begin{bmatrix} \overline{\mathcal{X}}_{k} \\ --- \\ \overline{\mathcal{U}}_{k|k} \end{bmatrix} \begin{bmatrix} \overline{\mathcal{X}}_{k} \\ --- \\ \overline{\mathcal{U}}_{k|k} \end{bmatrix}^T \right)^{-1}$$

completing the algorithm.